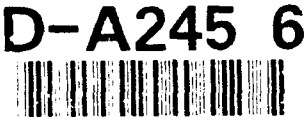

(2)

A TRIDENT SCHOLAR PROJECT REPORT

NO. 184

OPEN-WATER RESISTANCE AND SEAKEEPING CHARACTERISTICS OF SHIPS WITH ICEBREAKING BOWS

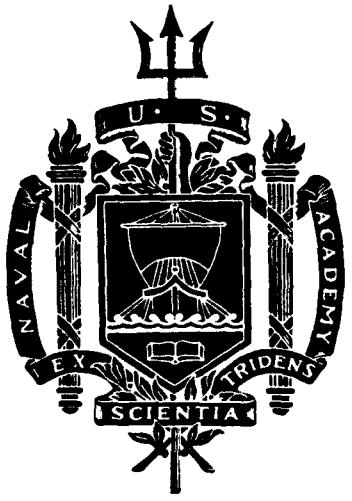

UNITED STATES NAVAL ACADEMY
ANNAPOLIS, MARYLAND

OPEN-WATER RESISTANCE AND SEAKEEPING CHARACTERISTICS OF SHIPS WITH ICEBREAKING BOWS

A Trident Scholar Project Report

by

Midshipman Casey J. Moton, Class of 1991

U.S. Naval Academy

Annapolis, Maryland

Advisors: Professor Roger H. Compton
Professor Bruce C. Nehrling
Naval Systems Engineering Dept

Accepted for Trident Scholar Committee

Francis D Connell
Chair

13 May 1991
Date

REPORT DOCUMENTATION PAGE

Form Approved
OMB No 0704-0188

1. AGENCY USE ONLY (Leave blank)	2. REPORT DATE	3. REPORT TYPE AND DATES COVERED
	13 May 1991	Final 1990/91

4. TITLE AND SUBTITLE
OPEN-WATER RESISTANCE AND SEAKEEPING CHARACTERISTICS OF SHIPS WITH ICEBREAKING BOWS

5. FUNDING NUMBERS

6. AUTHOR(S)
Casey J. Moton

7. PERFORMING ORGANIZATION NAME(S) AND ADDRESS(ES)
U.S. Naval Academy, Annapolis, MD

8. PERFORMING ORGANIZATION REPORT NUMBER
U.S.N.A. - TSPR; 184 (1991)

9. SPONSORING/MONITORING AGENCY NAME(S) AND ADDRESS(ES)

10. SPONSORING/MONITORING AGENCY REPORT NUMBER

11. SUPPLEMENTARY NOTES
Accepted by the U.S. Trident Scholar Committee.

12a. DISTRIBUTION/AVAILABILITY STATEMENT
This document has been approved for public release; its distribution is UNLIMITED.

12b. DISTRIBUTION CODE

13. ABSTRACT (Maximum 200 words)

Most research conducted on icebreaking ships has concentrated on their performance in ice fields. One area that has been neglected is the performance of such ships during their transit from their homeport to the ice field. The experimental research undertaken is intended to show how variation of icebreaking hull shape parameters will affect open-water powering and seakeeping performance. Based on a current U.S. Navy ice-capable ship hull form, a parent hull and four systematically varied hull forms were designed, fabricated, and tested in calm water and regular waves in the U.S. Naval Academy's Hydromechanics Laboratory 380-foot towing tank. Bow shape parameters considered to be of major importance for icebreaking--specifically, the waterline angle and the section flare angle at a point 10 % of the waterline length aft of the forward perpendicular--were varied over ranges dictated by current "good icebreaker practice." Calm water resistance as well as pitch, heave, relative vertical motion, and added resistance due to waves in long crested head seas were determined on the basis of model tests using eight foot long models.

14. SUBJECT TERMS
Ice-breaking vessels
Hulls (Naval architecture)
Ships--Seakeeping

15. NUMBER OF PAGES
102

16. PRICE CODE

17. SECURITY CLASSIFICATION OF REPORT	18. SECURITY CLASSIFICATION OF THIS PAGE	19. SECURITY CLASSIFICATION OF ABSTRACT	20. LIMITATION OF ABSTRACT
UNCLASSIFIED	UNCLASSIFIED	UNCLASSIFIED	

ABSTRACT

Most research conducted on icebreaking ships has concentrated on their performance in ice fields. One area of their operations which has been neglected is the performance of such ships during their transit from their homeport to the ice field. Powering requirements are dominated by resistance in ice, and, of course, seakeeping is of little importance in ice covered waters. The recent interest in "ice-capable" ships, with both a light icebreaking mission requirement and either a cargo-carrying or a research mission requirement, dictates that ships designed to meet such requirements have greater emphasis placed on their open-water transit characteristics.

The experimental research undertaken as the core of this Trident Scholar project is intended to show how variation of icebreaking hull shape parameters will affec open-water powering and seakeeping performance. Based on a current U.S. Navy ice-capable ship hull form, a parent hull and four systematically varied hull forms were designed, fabricated, and tested in calm water and regular waves in the U.S. Naval Academy's Hydromechanics Laboratory 380 foot towing tank. Bow shape parameters considered to be of major importance for icebreaking performance - specifically, the waterline angle and the section flare angle at a point 10% of the waterline

length aft of the forward perpendicular - were varied over ranges dictated by current "good icebreaker practice." Calm water resistance as well as pitch, heave, relative vertical motion, and added resistance due to waves in long crested head seas were determined on the basis of model tests using eight foot long models.

TABLE OF CONTENTS

LIST OF FIGURES

LIST OF TABLES

LIST OF SYMBOLS

AME ADVANCED MARINE ENTERPRISES, INC.

AP AFTER PERPENDICULAR

A_{WP} WATERPLANE AREA AT DESIGN WATERLINE

B BEAM

℄ BASELINE

B_{MX} MAXIMUM OVERALL BEAM

B_{WL} MAXIMUM BEAM AT DESIGN WATERLINE

℄ CENTERLINE

C_A CORRELATION ALLOWANCE

C_B BLOCK COEFFICIENT, $V/(L \times B_{WL} \times T)$

C_F ITTC 1957 FORMULATION FRICTIONAL RESISTANCE COEFFICIENT

C_{Fm} MODEL FRICTIONAL RESISTANCE COEFFICIENT

C_{Fs} SHIP FRICTIONAL RESISTANCE COEFFICIENT

C_P PRISMATIC COEFFICIENT, $V/(SA_X \times LWL)$

C_R RESIDUARY RESISTANCE COEFFICIENT, $C_T - C_F$

C_{Tm} MODEL TOTAL RESISTANCE COEFFICIENT

C_{Ts} SHIP TOTAL RESISTANCE COEFFICIENT

C_{VP} VERTICAL PRISMATIC COEFFICIENT, $V/(A_{WP} \times T)$

C_X MAXIMUM SECTION COEFFICIENT, $SA_X/(B_{WL} \times T)$

DWL DESIGN WATERLINE

EHP EFFECTIVE HORSEPOWER

F_b ICEBREAKING HULL PRESSURE COEFFICIENT

FP FORWARD PERPENDICULAR

FPS FEET PER SECOND

F_n FROUDE NUMBER

g ACCELERATION DUE TO GRAVITY

H HULL DEPTH, KEEL TO DECK-AT-EDGE

ITTC INTERNATIONAL TOWING TANK CONFERENCE

KM_L LONGITUDINAL METACENTRIC HEIGHT

KM_T TRANSVERSE METACENTRIC HEIGHT

k_{zz} YAW MASS GYRADIUS

L LENGTH

LCB LONGITUDINAL DISTANCE FROM AMIDSHIPS TO THE CENTER OF BUOYANCY

LCF LONGITUDINAL DISTANCE FROM AMIDSHIPS TO THE CENTER OF FLOTATION

LCG LONGITUDINAL DISTANCE FROM AMIDSHIPS TO THE CENTER OF GRAVITY

LOA LENGTH OVERALL

LPP LENGTH BETWEEN PERPENDICULARS

LWL LENGTH ALONG THE DESIGN WATERLINE

MIZ MARGINAL ICE ZONE

NAHL NAVAL ACADEMY HYDROMECHANICS LABORATORY

RAO RESPONSE AMPLITUDE OPERATOR

RBM RELATIVE BOW MOTION

R_n REYNOLDS NUMBER

R_T TOTAL RESISTANCE

SA_x MAXIMUM SECTIONAL AREA

$S_{1/3}$	AVERAGE OF 1/3 HIGHEST NUMERICAL VALUES
$S_{1/10}$	AVERAGE OF 1/10 HIGHEST NUMERICAL VALUES
SWH	SIGNIFICANT WAVE HEIGHT
T	DRAFT
TF	TRANSFER FUNCTION
TLR	TOP LEVEL REQUIREMENT
TSD	TECHNICAL SUPPORT DEPARTMENT
USNA	UNITED STATES NAVAL ACADEMY
V_m	MODEL VELOCITY
V_s	SHIP VELOCITY
α	WATERLINE ANGLE
β	FLARE ANGLE
η_1	ICEBREAKING COEFFICIENT
η_2	ICECUTTING COEFFICIENT
λ	SCALE FACTOR
μ_0	ICEBREAKING HULL EFFICIENCY
ϕ	STEM ANGLE
ρ	WATER DENSITY
⋈	AMIDSHIPS
Δ	DISPLACEMENT
∇	VOLUMETRIC DISPLACEMENT

1. INTRODUCTION

Icebreakers have long played a vital, yet to much of the world, overlooked role in maritime operations. Countries such as Canada and the Soviet Union have always recognized the importance of icebreakers, as many of their ports and coastal areas are ice-covered much of the year. Icebreakers are essential to the economic and military survival of such countries. The United States has recognized the importance of icebreakers. U.S. icebreakers have enabled the accomplishment of both commercial and military Arctic/Antarctic missions, research in ice-covered waters, search and rescue, and the maintenance of economic routes in the Northwest Passage, the Great Lakes, and many northern harbors.

Traditionally, designers of icebreakers have concentrated on the ship performance in an ice field. Hull forms are driven by the goal of improving ice-breaking capability, minimizing total resistance in ice, and lessening structural loads and damage due to ice impacts. After all, the primary mission of these ships is to break through ice. More recently, however, there have been needs identified requiring ships whose primary missions require the ability to perform unescorted missions in ice-covered waters - including platform supply and oceanographic research. The mission requirements of such ships often include operating in areas of lesser ice

thickness such as the Marginal Ice Zone (MIZ). These ships are normally homeported in distant U.S. ports and thus must make long open ocean transits to and from their ice-covered operating areas. These ships still must be designed to operate safely and effectively in ice, although the icebreaking requirements are less than those of the larger polar icebreakers. New concerns, specifically open water powering and seakeeping performance, move the designer to investigate ways to vary hull form so as to satisfy these operational concerns. To date, little research has been done to quantify how varying the hull form parameters which affect icebreaking will affect seakeeping and powering.

The goal of this project is to take a parent hull which is representative of ships that must both operate in ice and make long open water transits, and to perform model tests on a series of systematic shape variations of that parent. Tests were performed on the selected parent and four variations. These tests included effective horsepower (EHP) in calm open water, flow visualization in calm water, and seakeeping in head seas. Pitch, heave, added resistance due to waves, and relative bow motion at Station 2 (of 20) were measured in regular, long crested waves. The results for each model were analyzed and then compared.

2. BASIC ICEBREAKING THEORY

Icebreaker design, a small specialty within naval architecture, is a complex matter, and there are aspects and terms within it which may not be familiar to some naval architects. A brief introduction into the icebreaking process, and a look at a current method of quantifying some of the geometric characteristics of icebreaking hull forms is in order.

The process of icebreaking can be divided into two basic modes: the continuous mode and the ramming mode. In the continuous mode, the ship progresses at a relatively slow but steady forward speed, dependent largely on ice strength and thickness. Vertical accelerations are small, as are trim angles. The most characteristic feature of this mode is that icebreaking is performed by flexural bending of the ice along the entire forebody waterline from the stem to the section of maximum beam. As ice thickness increases, the ship begins to lose the capability to maintain a steady forward speed, and enters a transition into the ramming mode of icebreaking.

In the ramming mode, the icebreaker can no longer sustain constant speed. It first must back away from the ice, and then charge ahead towards the ice. As the stem strikes the ice, initial failure of the ice occurs by simple crushing. Then the raked stem of the icebreaker rides up onto the ice,

resulting in increasingly large bow up trim angles, and increased resistance to forward motion until progress stops. The ship's weight, applied to the ice at the stem of the icebreaker causes structural failure of the ice sheet. This failure usually results in both radial and circumferential breaks which result in floating ice fragments. The ship then backs away from the ice and repeats the process [1]. Figure 2-1 shows how ship velocity varies with ice thickness and indicates the approximate operational limits of the continuous and ramming modes.

Continuous mode performance is easier to analyze and describe due to its steady nature. Ramming mode performance is much more difficult to analyze due to its transient nature. Ramming mode analyses tend to be much more empirical and difficult to verify, while continuous mode analyses tend to be more theoretical and easier to substantiate.

Intuitively, the shape of an icebreaker's hull must have a large effect on its icebreaking capability. Fortunately, certain key hull form parameters have been shown to improve performance in both continuous and ramming modes. When considering these hull parameters, the important idea on which to focus is that the best hull form must maximize "the conversion of [forward] thrust into a combination of downward (to break, tip, and submerge the ice) and transverse (to move the ice out of the [ship's] path) forces."[2] Stem and

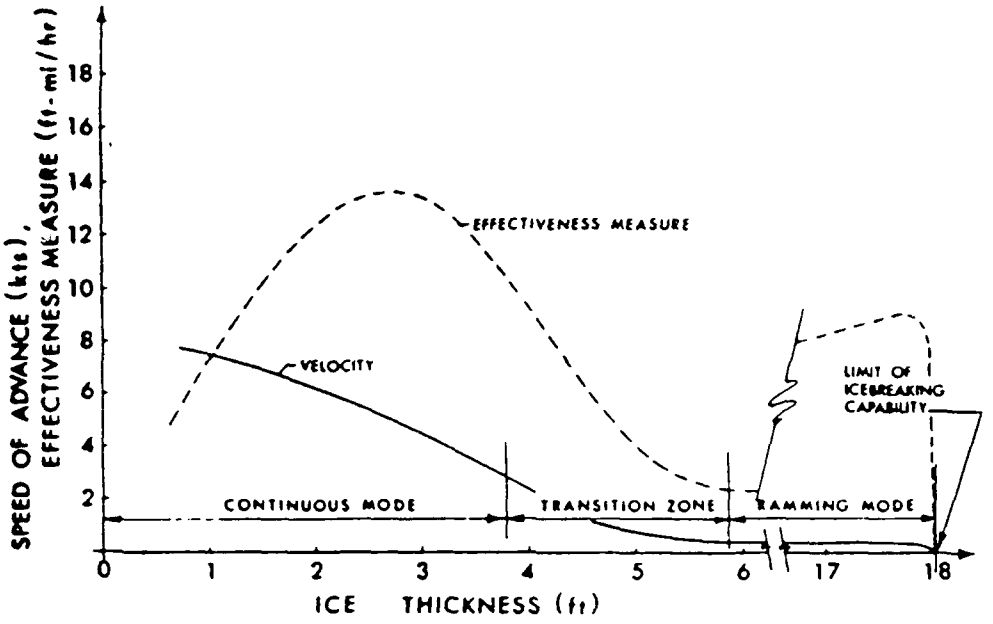

Figure 2-1, Icebreaker speed-of-advance as a function of ice thickness, showing relative importance of ice-breaking modes

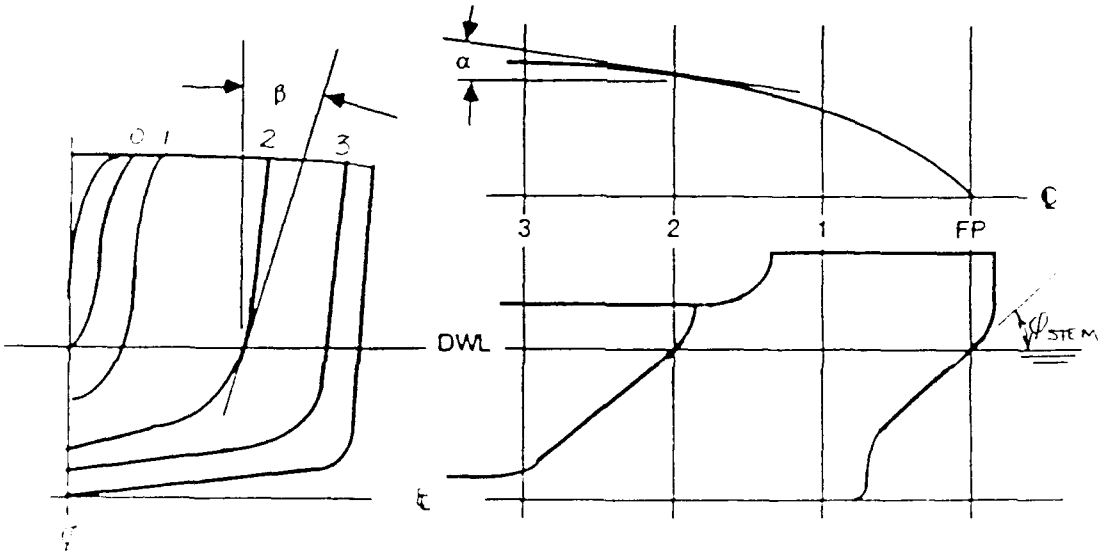

Figure 2-2
DEFINITION FOR HULL FORM BOW ANGLES

forebody form determine this capability more than any other parts of the hull. More displacement forward is an objective, especially when in the ramming mode. This is accomplished by designing the forebody of an icebreaker to be quite full. As a result, the center of buoyancy is rather far forward (relative to non-icebreakers), the station of maximum beam is usually well forward of amidships and entrance angles are quite large. This full forebody characteristic improves maneuvering, but may cause open water resistance to increase sharply and may affect seakeeping performance.

The stem angle of the ship plays an important role in icebreaking, primarily in the ramming mode. In particular, when a ramming attempt is unsuccessful, the ship will have to use its engines to extract itself from the ice. Stem angle plays a major role in determining the extraction force magnitude.

The stern and afterbody have little effect on the normal icebreaking capability of the ship. The primary design concerns are (1) preventing ice chunks from flowing into the rudders, screws and after appendages, where they may cause serious damage and (2) shaping the stern such that astern operation into broken ice will not result in damage or lack of ship control/mobility when backing down.

The major goal of this study is to provide guidance to the designer relative to the tradeoffs between continuous mode icebreaking and open ocean performance as they are affected by

bow shape. Two Soviet naval architects, Shimansky and Kashteljan, have developed and published a widely accepted method of predicting icebreaker performance in the continuous mode icebreaking. Shimansky began the work by defining coefficients dependent on forebody form and relating them to total downward force and the ability to break ice. Kashteljan then used the coefficients in a method to predict the resistance of a ship while actually breaking ice. These coefficients are dependent on two hull form angles, the flare angle, β, and the waterline angle, α. Both of these, and the stem angle, ϕ, are defined in Figure 2-2. The first coefficient, η_1, is the icebreaking coefficient, which relates the total vertical force to the total longitudinal force. The second coefficient is η_2, the icecutting coefficient, which relates total transverse force to the total longitudinal force. These coefficients are defined as follows [3]:

$$\eta_1 = \frac{\int_0^m \frac{\tan\alpha\tan\beta\,(1+\tan^2\alpha)^{1/2}}{1+\tan^2\alpha+\tan^2\beta}\,dx}{\int_0^m \frac{\tan^2\alpha\,(1+\tan^2\alpha)^{1/2}}{1+\tan^2\alpha+\tan^2\beta}\,dx} \qquad (1)$$

$$\mu_0 = (1+1/\eta_1) \qquad (2)$$

Here, μ_0 is hull efficiency, dependent only on the icebreaking coefficient. The coefficients may be calculated

$$\eta_2 = \frac{\int_0^m \frac{\tan\alpha\,(1+\tan^2\alpha)^{1/2}}{1+\tan^2\alpha+\tan^2\beta}\,dx}{\int_0^m \frac{\tan^2\alpha\,(1+\tan^2\alpha)^{1/2}}{1+\tan^2\alpha+\tan^2\beta}\,dx} \qquad (3)$$

by integrating expressions involving the flare and waterline angles from the forward perpendicular to the station of maximum beam, m. μ_0 and η_2 are the two coefficients commonly calculated to facilitate comparisons of different icebreaker hull forms. Recommended values for these coefficients are 1.4 and 3.0, respectively [4]. Any hull having coefficients close to these is considered to have good continuous icebreaking characteristics.

Shimansky's coefficients, and Kashteljan's method, are the generally accepted standard for predicting force relationships and resistance in continuous mode icebreaking. Kashteljan's algorithm is especially useful because it accounts for ship size, bow form, velocity, ice strength and ice thickness. The correlation between the predicted resistance using Kashteljan's method and full scale results from tests involving the icebreakers MOBILE BAY and KATMAI BAY are very close, verifying the validity of his arguments, and, more importantly for this project, the significance of the coefficients μ_0 and η_2 [5]. By determining the value of these coefficients for each hull, one can postulate that the series hull forms represent acceptable shapes for icebreaking ships.

3. PARENT HULL SELECTION AND BOW FORM VARIATION

After formulation of the problem, the first major task was to identify the important hull form characteristics of icebreakers. Knowing these characteristics, a parent hull form could be selected and defined by a standard lines drawing. Once a parent form was selected, the nature of the systematic variation of the parent was determined. The systematic series was limited by the practical constraints of time and money to four variants and the parent.

Selection of the parent hull form was done both through analysis of icebreaking related literature and through consultation with Mr. Peter Zahn, of Advanced Marine Enterprises (AME), and Mr. Daniel Bagnell, of Band Lavis and Associates, both of whom have extensive experience in designing U.S. Coast Guard and U.S. Navy icebreakers and MIZ ships. The desired hull form was to have a mission which required light ice operation, but which also included long open ocean transits from its homeport to the MIZ operational area. The parent was to be representative of such ships, with no unusual features which would lessen the general usefulness of the performance data acquired from the model tests. In addition, there were to be no special appendages which might mask the effects of basic hull shape on open water performance. Thus, propeller shaft bossings, skegs, rudders,

and special stem forefoot shapes were not included in the shapes tested.

To ensure that the parent and its variants satisfied the light icebreaking requirement, research was done to determine ranges of hull parameters typical to icebreakers. L.C. Melberg, et. al [6], suggest "good practice" limits on the following design variables for polar icebreakers:

$$3.5 < L/B < 5.0$$
$$2.1 < B/T < 3.7$$
$$0.42 < C_B < 0.69$$
$$0.57 < C_P < 0.70$$

As far as bow form angles, defined earlier in Figure 2-2 are concerned, Kashteljan suggested the following values, which are consistent with classical Soviet practice [7]. The stem angle, ϕ, defined with respect to the design waterline, is generally near 30°. The flare angle, β, is near 45° for medium and heavy icebreakers, but often less for auxiliary icebreakers. The waterline angle, α, generally should fall between 24° to 30° for icebreakers.

Most icebreakers have a longitudinal center of buoyancy (LCB) forward of amidships, and a station of maximum beam as far forward as possible while still maintaining reasonable waterline angles. This places the center of gravity forward and thus facilitates the icebreaking process. Icebreakers often have a prominent forefoot (as in Figure 3-1) which is especially useful in the ramming mode of icebreaking. Such a knuckle in the stem prevents the bow from riding so far onto the ice that extraction becomes extremely difficult barring

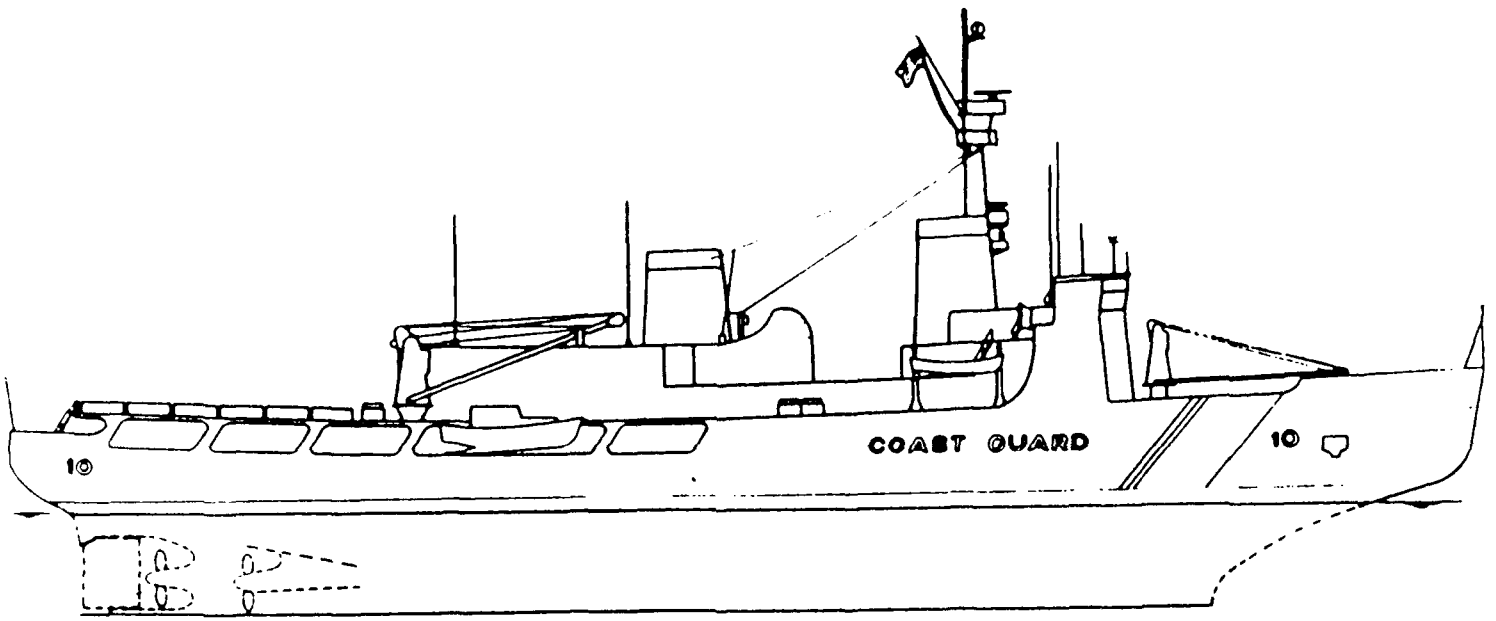

Figure 3-1, A knuckled forefoot at the stem on the POLAR Class Icebreaker

failure of the ice, or, the loss of stability when effectively grounded becomes a concern.

It was decided that a suitable mission, representative of those requiring light icebreaking and efficient open-water transits, was oceanographic research in the MIZ. The hull form requirements dictated by the oceanographic research mission included a large after deck area to facilitate over-the-stern research. This requirement, in turn, results in providing a flat, transom stern. Most ships of this type have twin screws and rudders for good low speed maneuverability and station keeping.

A list of general hull characteristics for the parent form was drafted. The MIZ oceanographic research ship with light icebreaking capabilities should have:

1. Twin screw, twin rudder
2. Transom stern, with large after deck area
3. L/B of around 5, in the higher limits of the icebreaking range, but the middle of the research ship range, with LWL about 300 feet
4. C_B of about 0.6
5. Forebody angles (α,β,ϕ) in the general icebreaker range
6. No forefoot knuckle

Several different hull forms were considered, again with the practicing icebreaker naval architects, Mr. Zahn and Mr. Bagnell. Among the hull forms considered were the POLAR Class, the Japanese SHIRASE, the DDI icebreaker, the BAL #77 icebreaker, and a planned ice-capable research ship for the National Science Foundation (NSF). Because none of the foregoing icebreakers had an oceanographic mission requirement

besides the NSF ship, their sterns were of conventional cruiser form, and thus had insufficient after deck area and excessive freeboard aft. Most fell within the overall hull parameter value ranges, and all represent "currently accepted practice." The NSF design was considered unacceptable from a powering standpoint because of the excessive slope of the afterbody buttocks.

A practical consideration in adopting a parent hull form was the availability of good hull geometry definition, i.e., the hull lines drawing. With the requirements to design five systematically related hulls and to fabricate them within a severely constrained time period so that tank testing in all five could be performed, the use of an automated (computer-aided) means of lines development was necessary. Ideally, a hull form already defined in FASTSHIP, the automated hull geometry package in use at the U.S. Naval Academy, would greatly facilitate both the model fabrication and the systematic variation of the forebody shape for other members of the series.

Perhaps purely serendipitously, the search for a current icebreaker design to use as a parent led to the FY92 T-AGS OCEAN (ICE), an ice-capable oceanographic survey ship designed to satisfy mission requirements developed by the Oceanographer of the Navy. The resulting ship design featured twin screws, twin rudders, a transom stern and large deck area aft for oceanographic research. The ship's mission required it to

make long open-water transits ending in operations in the MIZ. The ship had a large amount of parallel midbody (30% LPP), a tight bilge radius joining sides of approximately constant slope with a constant 15° deadrise bottom, low freeboard aft (advantageous for research), and a station of maximum beam forward of amidships. In addition, hull parameters fell within the accepted range of light icebreaking, or ice-capable ships, with a L/B of 5.48, a LWL of about 318 feet, a stem angle of 36°, a waterline angle of 20.5°, and a flare angle of 24.5° at Station 2 (10% LPP back from the forward perpendicular). Parameters slightly outside of the acceptable range for most icebreakers were rationalized since the classical values were given for medium and heavy icebreakers. This ship will be a light icebreaker, intended to break a maximum of three feet of first-year ice, an MIZ characteristic. The T-AGS OCEAN (ICE) design has no knuckled forefoot. Finally, besides being a ship incorporating the kind of compromises necessary between icebreakers and research-oriented ships, the preliminary lines were available from Advanced Marine Enterprises (AME) as a FASTSHIP surface file. A reduced scale lines plan of the T-AGS OCEAN (ICE) parent after final fairing at the U.S. Naval Academy is shown in Figure 3-2. Also, a report detailing the "Feasibility Studies for an Ice Capable Oceanographic Research Survey Ship - FY92 T-AGS OCEAN (ICE)" by Strasel, et. al, covers many of the operational characteristics and requirements of the parent hull [8].

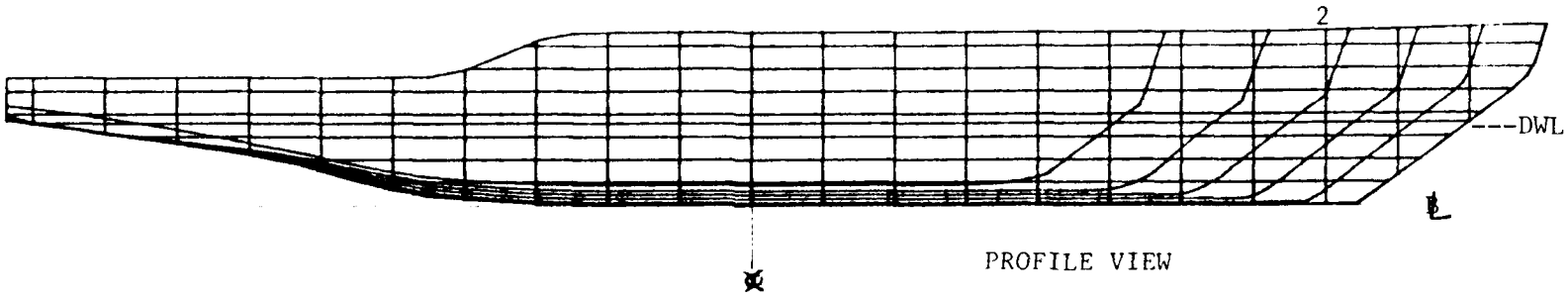

PROFILE VIEW

FIGURE 3-2, Lines Plan

T-AGS OCEAN (ICE)

Parent Hull Form
(Scale 1:500)

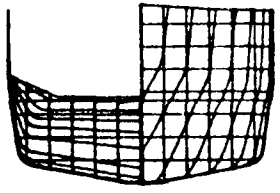

BODY PLAN

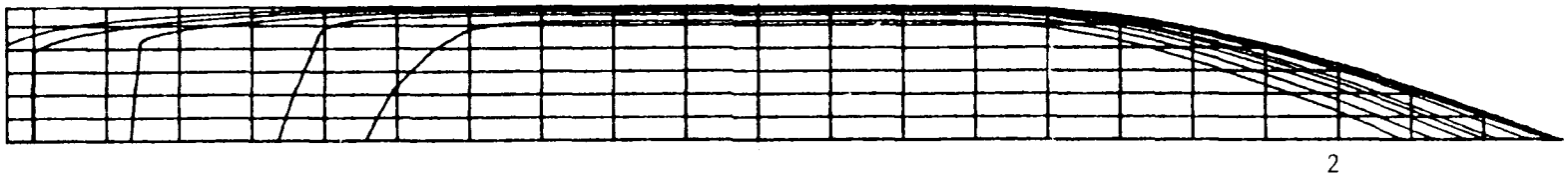

HALF-BREADTH PLAN

Once the parent was chosen, the next major task was to decide upon the hull parameters to be varied, the ranges of the variations, and those parameters to be held constant. Again, the only practical restriction was that four variations could be designed, built, and tested plus the parent within the limited time available. Logically, the number of parameters to be varied systematically needed to be low, so that it would be possible to isolate the effects of the variations. In addition, it was desirable to select parameters considered to be important to the icebreaking performance of the ship.

After studying much of the current literature on icebreaking hull forms, it was decided that the two most important and reasonable values to vary were the flare angle, β, and the waterline angle, α, as defined in Figure 2-2 at a point 10% of LPP aft of the forward perpendicular (Station 2) at the design waterline. All of the references cited indicated that these values were the best ones to mathematically quantify the continuous mode icebreaking effectiveness of a ship, both in relation to its resistance in ice and its icebreaking capability. Specifically, Kashteljan's widely accepted icebreaker design methods use these angles in icebreaking resistance equations, in the form of the coefficients, μ_0 and η_2. One side effect of the importance placed on these two angles is also noteworthy: a large data base exists for various icebreakers. A primary

consideration in their variation was that they should not go so far as to cause doubts as to the icebreaking performance of the systematically varied hull forms. This was particularly important as ice testing of models is beyond the technical scope of this project. Such testing is not within the capabilities of the U.S. Naval Academy Hydromechanics Laboratory.

Once the decision to vary these angles was made, it was necessary to define a range over which they would be varied. Again the objectives were to modify them in a systematic manner, with changes large enough to be noticeable, but not so large that they placed the hull form out of normal icebreaking ranges. Advanced Marine Enterprises (AME) provided information [9] which correlates good hull angles with ice loading, under the assumption that the loading is a function of a pressure coefficient, Fb, which is a function of α and β. Assuming that reduced hull loads are a desirable characteristic of an ice capable hull, it is desirable to reduce Fb as much as possible. A value of Fb = 1.00 is taken to represent the nominal value of the pressure coefficient and any combination of α and β yielding Fb = 1.00 would also be nominal. Figure 3-3 presents a plot of Fb = 1.00 versus both α and β. Values of α and β at 10% LPP aft of the FP for some "heavy" icebreakers are plotted to define the full end of the reasonable range of these angles. The box on this curve defines the traditional ranges of Soviet design practice.

Optimum Pressure Coefficient (Fb=1)

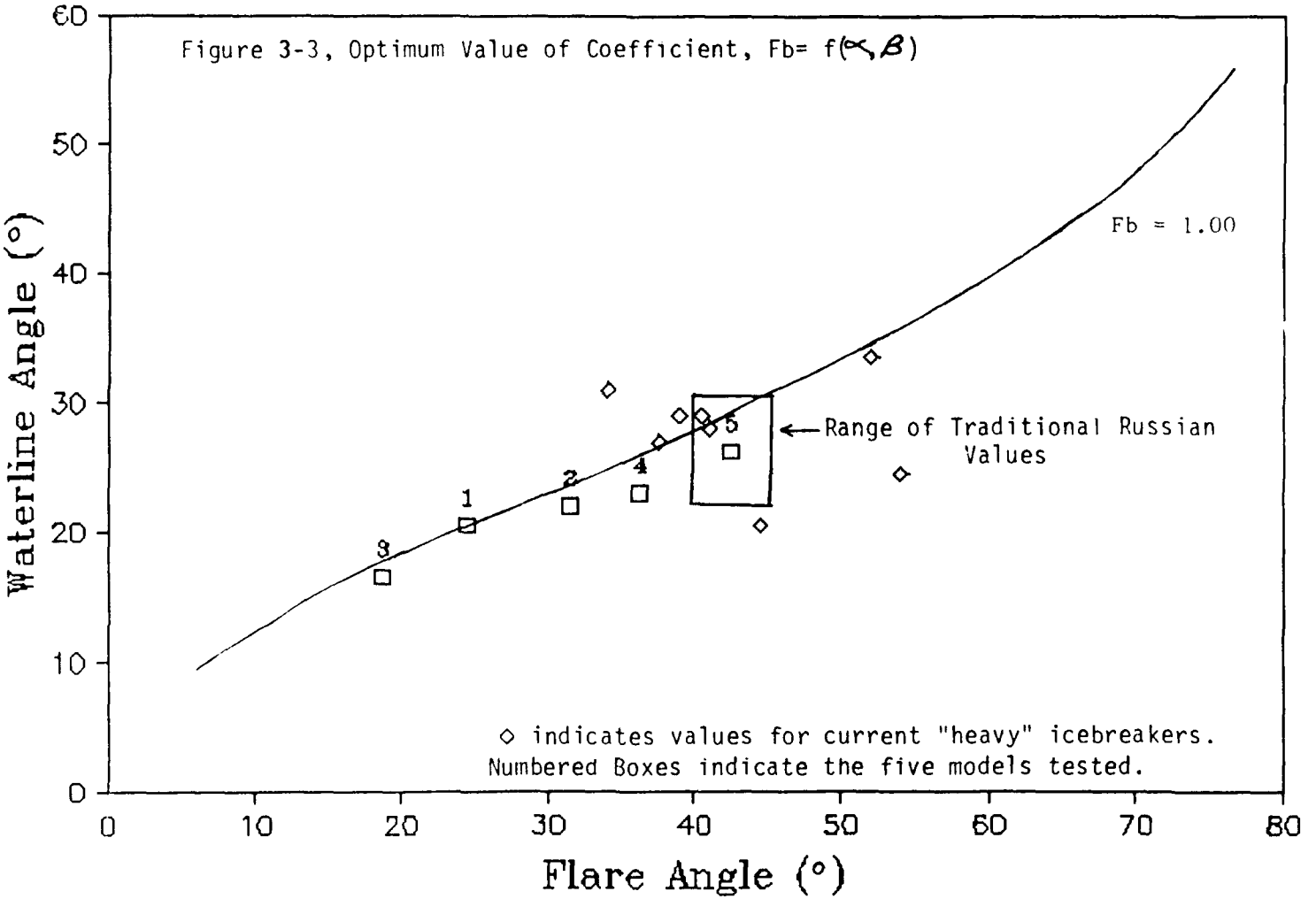

Placing one of the four variants within this box was desirable. It is not the purpose of this graph to provide the only feasible combinations of these bow form angles. It is intended to provide a reasonable curve along which values of α and β could be chosen, while maintaining them in a range where the icebreaking effectiveness can not be strongly doubted. Figure 3-3 also shows the parent hull form and the four different combinations of α and β which were chosen as the tested modifications. Three of the bow variants had angles larger than the parent, while one (Bow 3) had lower values. As a rule, ships intended for heavy icebreaking have larger values of α and β, while light icebreakers (or even non-icebreakers) have lower values.

The previously mentioned FASTSHIP hull definition program was used in the bow variation process. While the angles could be changed to the predetermined values, other characteristics of the hull should, as much as possible, remain constant. These "constant" characteristics were the draft, waterline length, maximum sectional area (and shape), and the afterbody (aft of Station 9). In addition, all models were ballasted so as to have zero static trim. By using a common afterbody, any effects of the afterbody on the open-water performance could be disregarded in a comparative analysis. Figure 3-4 shows the lines of the common afterbody which was present for all models. AME provided the initial surface file for the parent hull form during the summer of 1990. Final fairing was done

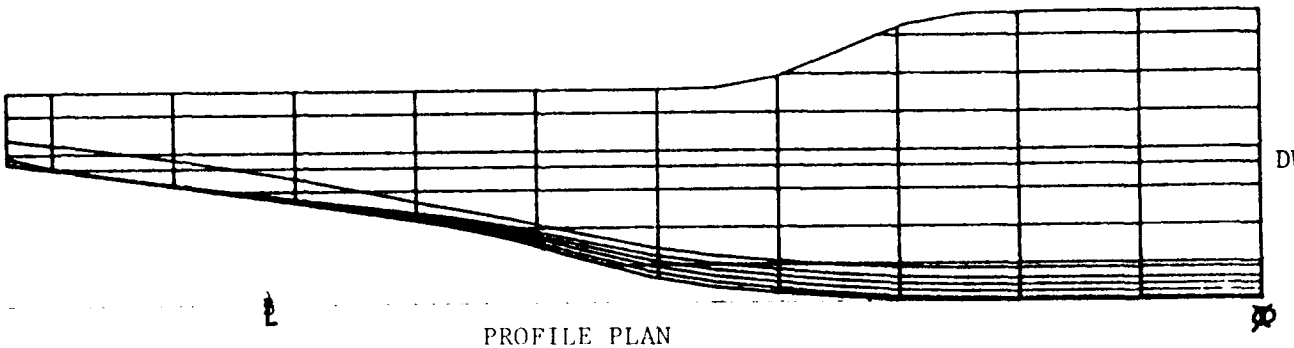

PROFILE PLAN

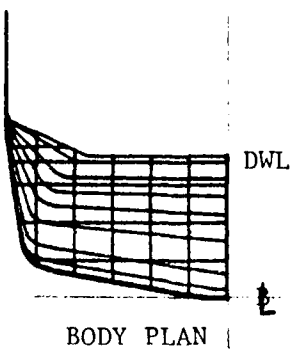

BODY PLAN

FIGURE 3-4, Lines Plan

Common Afterbody Section
(Scale 1:300)

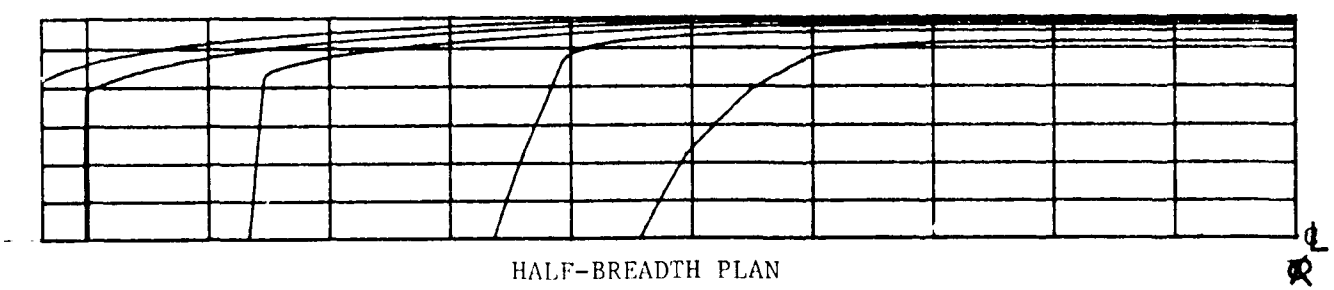

HALF-BREADTH PLAN

on the file at the U.S. Naval Academy. The hull form was split into two different surfaces - an afterbody section (from Station 9 to the stern) and a forebody or bow section. Onecommon afterbody and five bow models were to be constructed. By so doing, only the geometric changes in the forebodies would be affecting the performance of the hulls. Extreme care in fairing all forebodies and the common afterbody at their common interface at Station 9 was necessary. Not only the same cross section shape was required, but, also, continuity of longitudinal hull slopes and curvature must exist across the joint at Station 9. It should be noted that, although FASTSHIP facilitated the hull fairing process overall, taking an already designed and faired surface file and attempting to force the flare and waterline angles to set values while refairing the hull was a difficult process. FASTSHIP was not designed for such a specialized application as this, and the added geometric restriction imposed by the intersection at Station 9 made the task even more difficult.

Figures 3-5 through 3-9 show the lines for each of the series forebodies. Bow 1 was the parent. Bow 2 had the next larger values of α and β. The change in the angles did not cause great difficulty in fairing for this bow. The only change was a slightly different stem angle, which resulted in a small increase in LWL of about 0.05 inches for the model. Bow 3 was the only forebody with smaller values of α and β

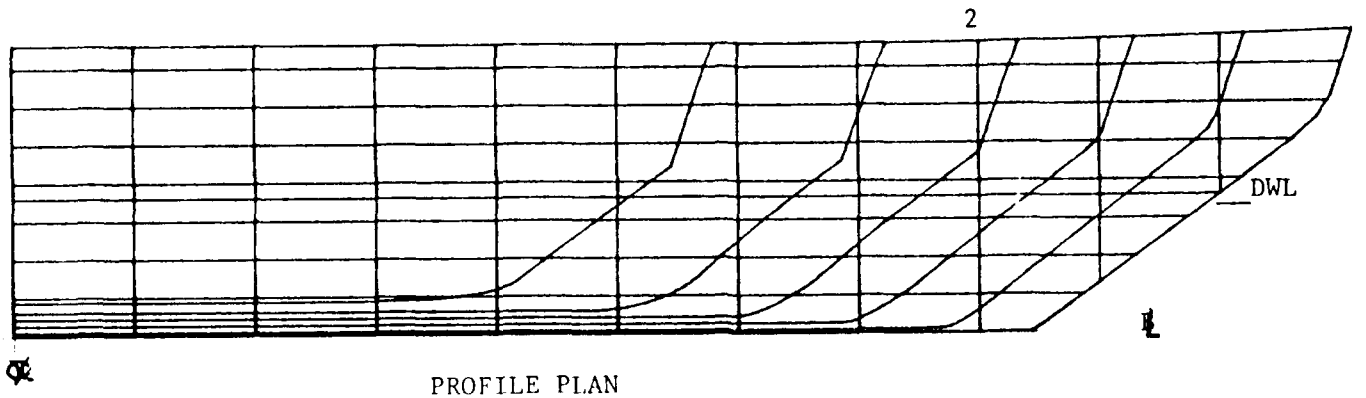

PROFILE PLAN

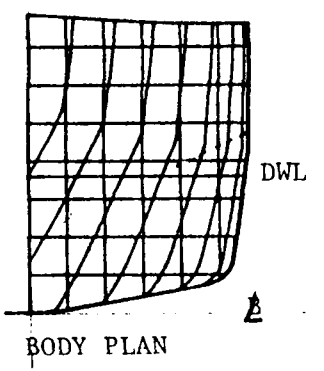

BODY PLAN

FIGURE 3-5, Lines Plan

Forebody, Bow 1 (Parent)
(Scale 1:300)

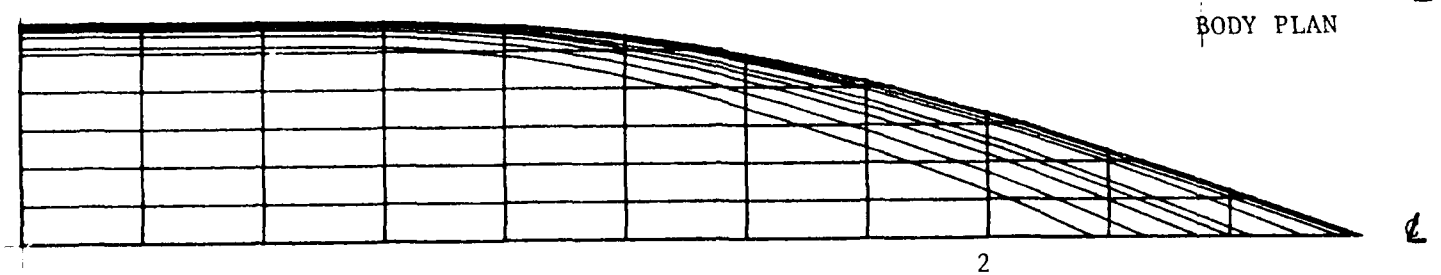

HALF-BREADTH PLAN

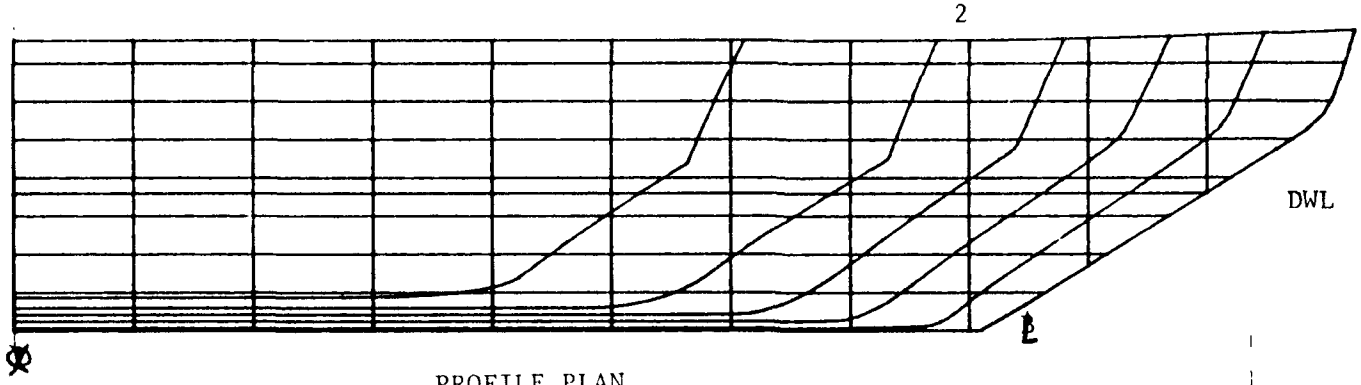

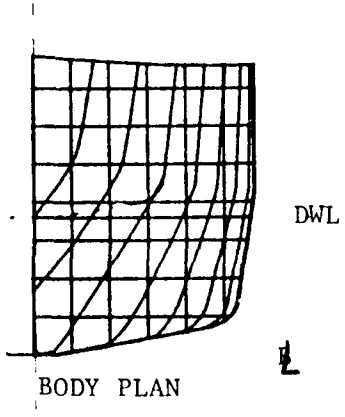

FIGURE 3-6, Lines Plan

Forebody, Bow 2
(Scale 1:300)

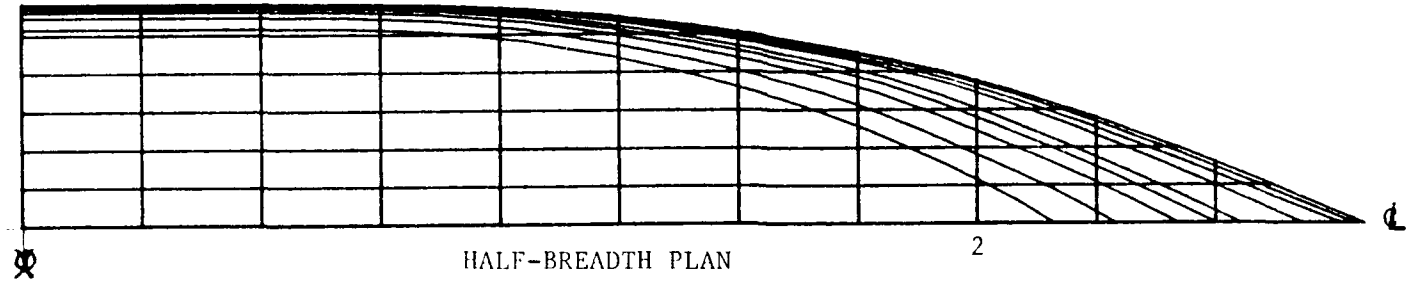

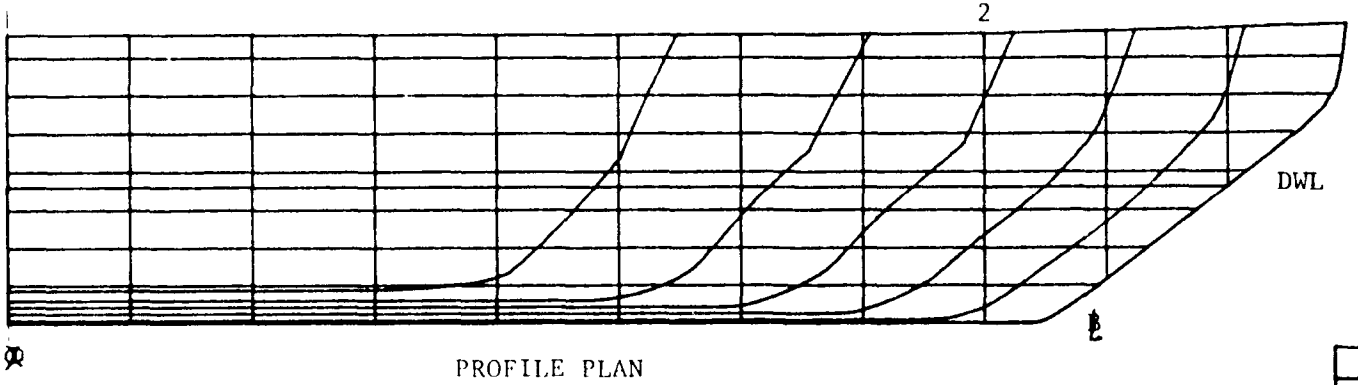

PROFILE PLAN

FIGURE 3-7, Lines Plan

Forebody, Bow 3
(Scale 1:300)

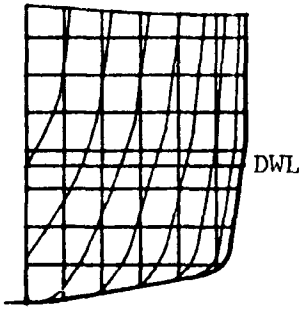

BODY PLAN

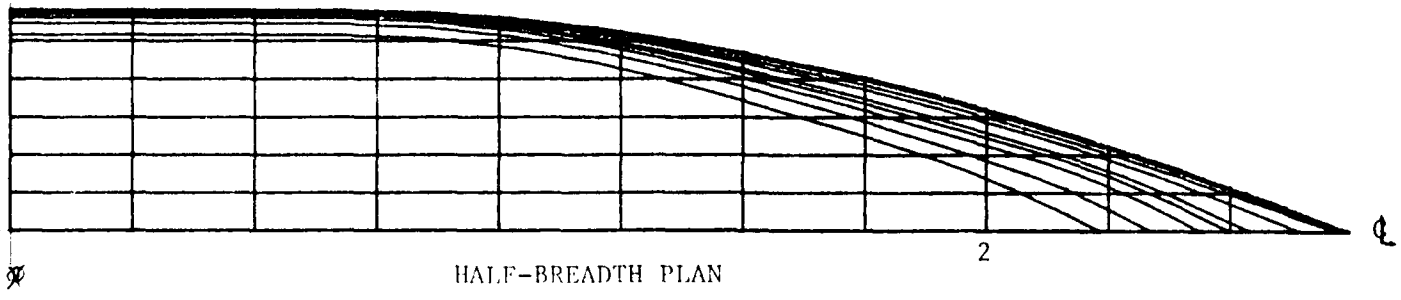

HALF-BREADTH PLAN

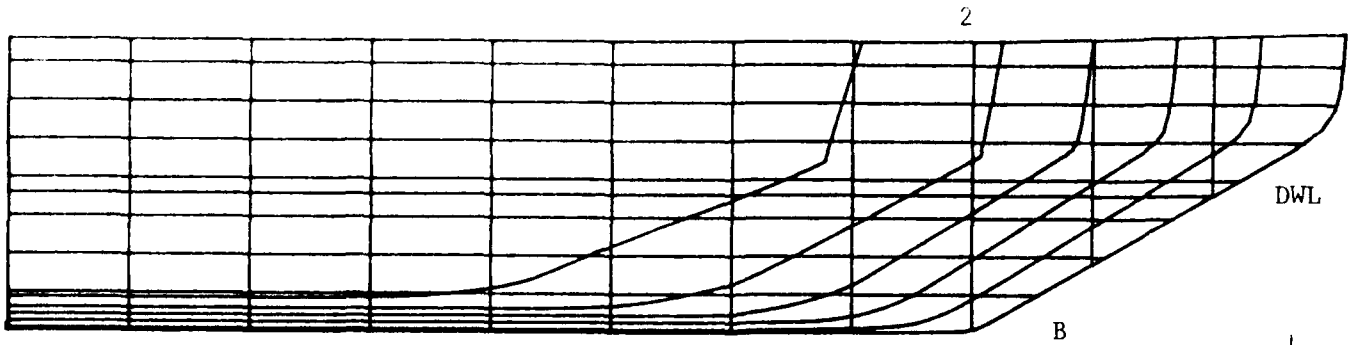

PROFILE PLAN

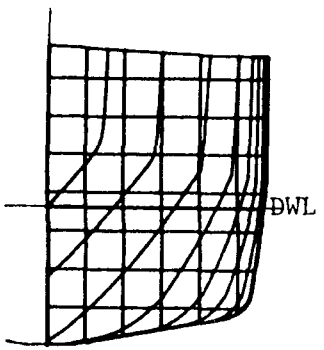

BODY PLAN

FIGURE 3-8, Lines Plan

Forebody, Bow 4
(Scale 1:300)

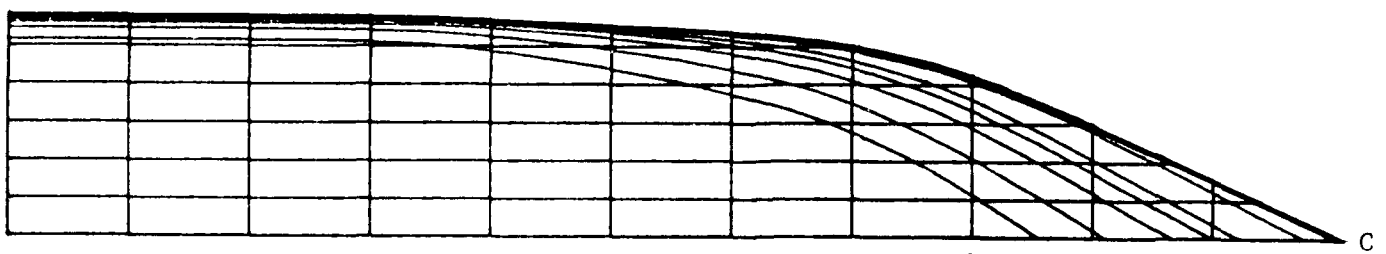

HALF-BREADTH PLAN

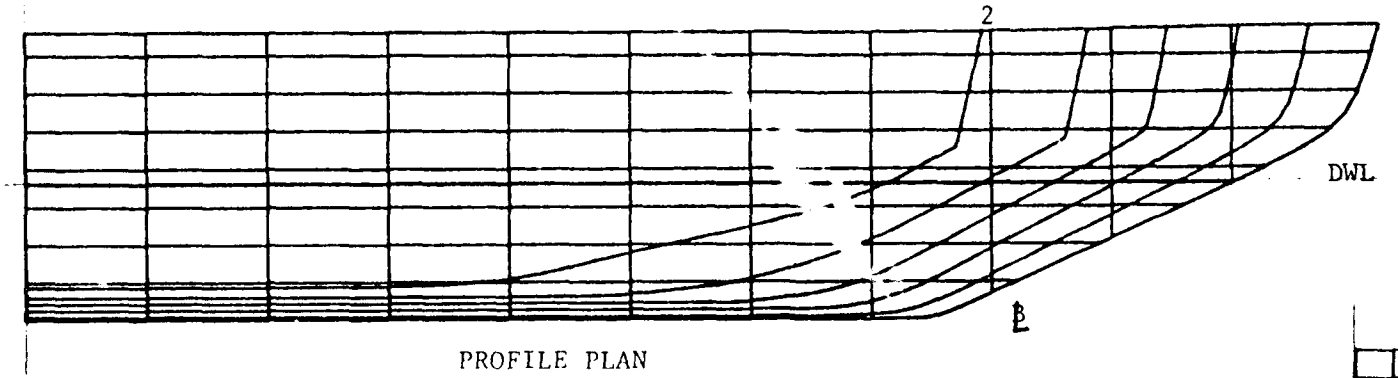

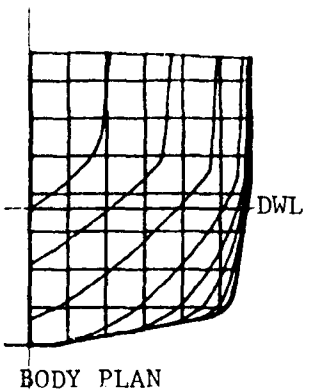

FIGURE 3-9, Lines Plan

Forebody, Bow 5

(Scale 1:300)

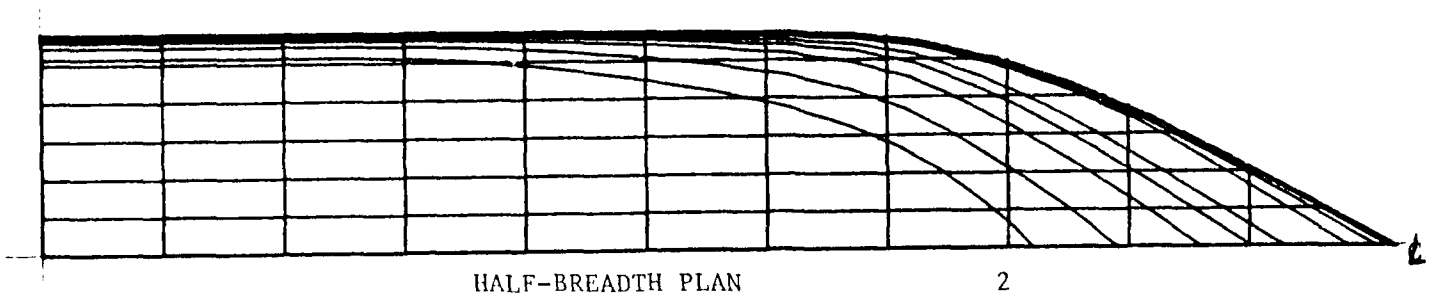

than the parent. As with Bow 2, fairing using FASTSHIP resulted in a similar change in stem angle, and a slight decrease in LWL (0.04 inches for the model). Bow 4 had values of α and β which were large enough to cause new problems in fairing. For both Bow 4 and Bow 5, the LWL was kept constant, but the location of the station of maximum waterline beam was extended forward somewhat to enable the increases in α. Bow 5 was the final bow, with the largest values of α and β. With Bow 5 faired, the resulting hull shape fell within the recommended ranges for α and β established for Soviet icebreakers. The station of maximum beam was even farther forward to fair the hull with the new required α, while the beam almost to the FP had to be increased at the waterline to enable the large β value. It is noted that these non-systematic hull changes were introduced only if absolutely necessary to fair in the angles for that bow. In addition, any local unfairities in the lines are practically unavoidable when using FASTSHIP in such an unconventional manner. Such slight areas of unfairness were resolved in the as-built models by close interaction with the model maker during the final hand fairing process.

Figure 3-10 presents the values of the two Shimansky coefficients for each bow modification, calculated using the sets of values of α and β at equal length intervals from the FP to the station of maximum beam as measured from the model lines plans. Also plotted are the values of the coefficients

Shimansky Coefficient Comparison

Sample: 23 Icebreakers

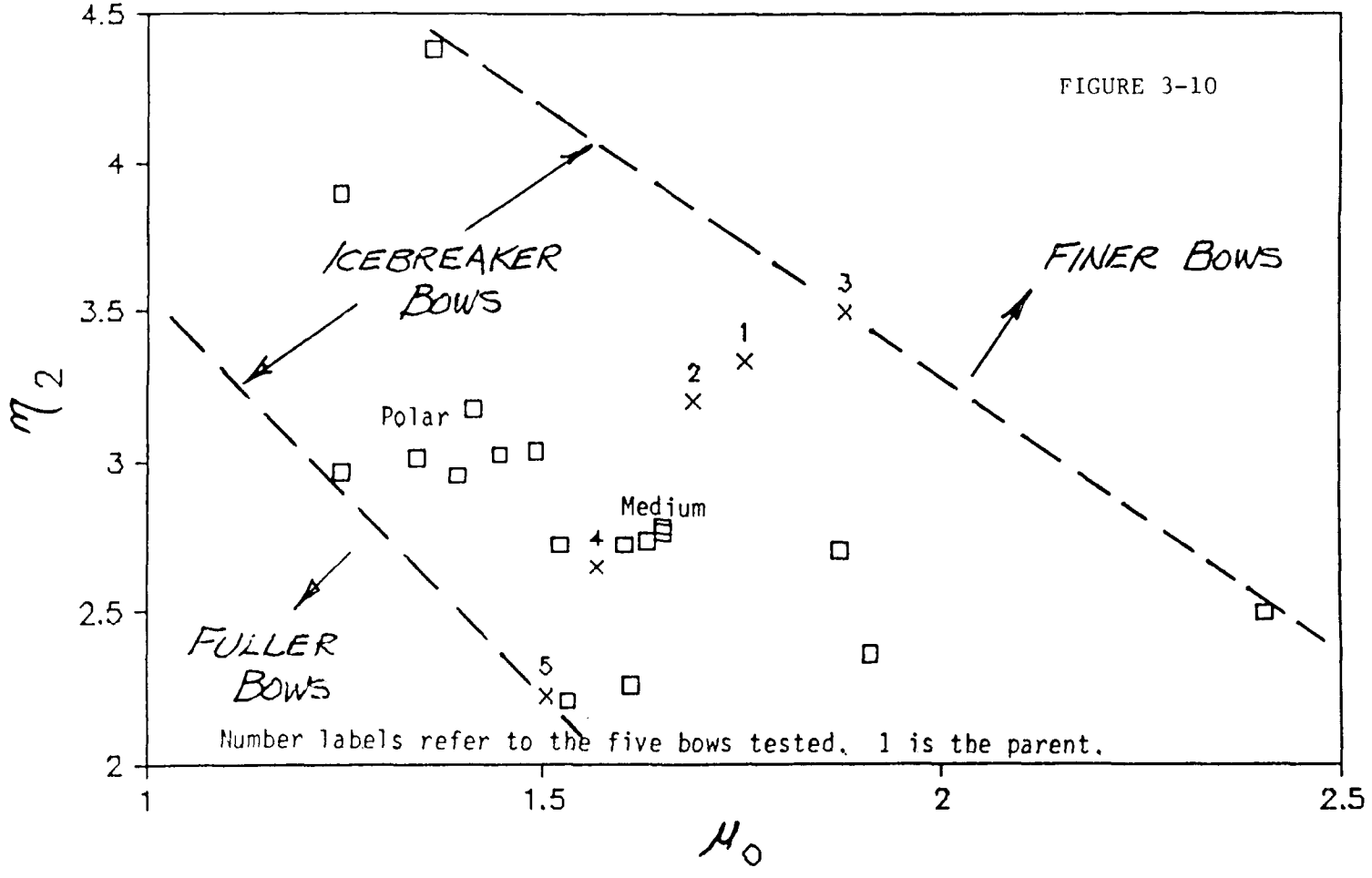

FIGURE 3-10

for many other icebreakers. This figure confirms that in no case did any of the series hull forms exceed normal icebreaker ranges. Bow 1's coefficients place it in the light icebreaking category. Bow 2 and Bow 3, as expected since their angle variations from the parent are the least, fall fairly close to Bow 1. Bow 4 and Bow 5, due to their larger bow angles and their increased beam in the forebody, are much nearer the normal icebreaker range. Bow 4 falls among medium icebreakers, some of which operate on the Great Lakes, including the WIND Class, the GLACIER, and the MACKINAW. Bow 5 falls near other heavier icebreakers, including the PIERRE RADISSON hull form.

A summary of model shape parameters is provided for all bows in Table 3-1, including the Shimansky coefficients and the bow angles, α and β. The expanded ship parameters, with a scale factor, λ, of 39.75 are presented in Table 3-2.

After final lines preparation, FASTSHIP was used to create numerical data files for each surface. These files were used to interface with the numerically controlled (NC) milling machine in the model shop of the U.S. Naval Academy's Technical Support Department (TSD). The desired molded hull shape was physically defined by waterline cuts spaced no more than a quarter inch apart over the entire length of the models. All hulls were milled from blocks of high density, closed cell foam. Figure 3-11 shows Bow 5 after the final waterline cuts were made by the NC mill machine. Each hull

TABLE 3-1, Model Parameters (λ=39.75)

		Bow 1	Bow 2	Bow 3	Bow 4	Bow 5
LPP (ft)		8.011	7.957	8.052	8.011	8.016
LOA (ft)		8.584	8.584	8.584	8.584	8.635
B_{wl} (ft)		1.433	1.433	1.433	1.433	1.433
B_{mx} (ft)		1.459	1.459	1.459	1.459	1.459
∇ (ft^3)		2.998	3.001	3.018	3.065	3.096
Δ (lb)$^+$		186.66	189.99	188.04	190.99	192.91
WSA (ft^2)		13.305	13.244	13.377	13.416	13.513
LCB* (in)		1.202	1.205	1.470	1.854	2.125
Kzz (ft)		2.003	1.989	2.013	2.003	2.004
LCF* (in)		-4.854	-4.604	-4.764	-3.517	-2.687
Awp (ft^2)		9.709	9.774	9.712	10.056	10.282
C_B		0.577	0.581	0.577	0.590	0.595
C_p		0.673	0.678	0.674	0.688	0.694
C_{WP}		0.846	0.857	0.842	0.876	0.895
C_x		0.858	0.858	0.858	0.858	0.858
C_{VP}		0.682	0.678	0.686	0.673	0.665
KM_T (ft)		0.293	0.298	0.286	0.311	0.329
KM_L (ft)		13.234	13.429	13.293	14.111	14.700
β_{Sta2} (°)		24.5	31.5	18.75	36.25	42.5
α_{Sta2} (°)		20.5	22.0	16.5	23.0	26.25
ϕ (°)		36	31.5	36.5	29.5	23.5
μ_0		1.751	1.658	1.877	1.566	1.503
η_2		3.331	3.199	3.492	2.644	2.223

+ Δ: in Fresh Water, Tank test temp.
* LCB, LCF: + forward amidships

TABLE 3-2, Ship Parameters

		Bow 1	Bow 2	Bow 3	Bow 4	Bow 5
LPP (ft)		318.42	316.32	320.05	318.42	318.63
LOA (ft)		341.21	341.21	341.21	341.21	343.25
B_{wl} (ft)		56.97	56.97	56.97	56.97	56.97
B_{mx} (ft)		58.00	58.00	58.00	58.00	58.00
∇ (ft^3)		188294	188505	189526	192494	194454
Δ (LTSW)+		5378.8	5384.9	5414.0	5498.8	5554.8
WSA (ft^2)		21023	20926	21136	21198	21352
LCB (ft)*		3.98	3.99	4.87	6.14	7.04
Kzz (ft)		79.61	79.07	80.01	79.61	79.66
LCF (ft)*		-16.08	-15.25	-15.78	-11.65	-8.90
Awp (ft^2)		15341	15444	15345	15890	16247
C_B		0.577	0.581	0.577	0.590	0.595
C_p		0.673	0.678	0.674	0.688	0.694
C_{WP}		0.846	0.857	0.842	0.876	0.895
C_x		0.858	0.858	0.858	0.858	0.858
C_{VP}		0.682	0.678	0.686	0.673	0.665
KM_T (ft)		11.66	11.86	11.35	12.38	13.09
KM_L (ft)		526.04	533.81	528.39	560.09	584.34
β_{Sta2} (°)		24.5	31.5	18.75	36.25	42.5
α_{Sta2} (°)		20.5	22.0	16.5	23.0	26.25
ϕ (°)		36	31.5	36.5	29.5	23.5
μ_0		1.751	1.658	1.877	1.566	1.503
η_2		3.331	3.199	3.492	2.644	2.223

+ Δ: in Salt Water, 59°F
* LCB, LCF: + forward amidships

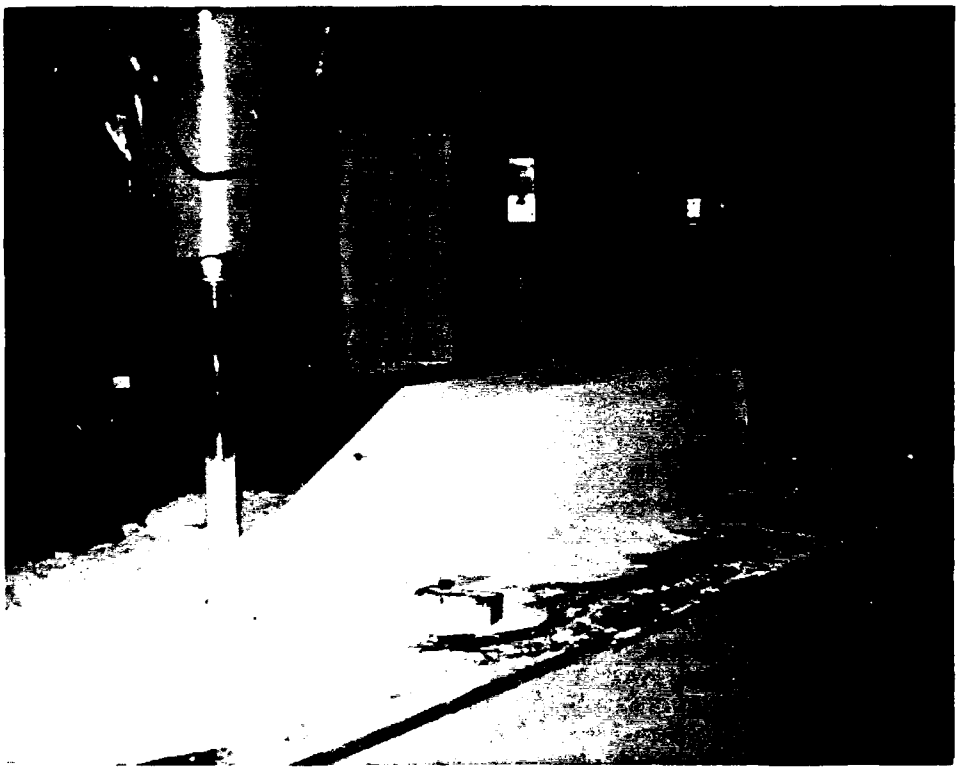

Figure 3-11, Bow 5 After Numerically Controlled Milling.

section was lightened by removing much of the interior foam to permit the installation of dynamometry needed for testing. Hull rigidity was provided by a wooden box structure installed within each section. After the milling of each surface, the hull sections were faired by hand, using the appropriate lines plan as the reference. At this point, all local unfairities which resulted from the unorthodox application of FASTSHIP (see above) were removed. After fairing, each surface was coated with a thin layer of epoxy and light fiberglass cloth to provide surface toughness. Then each section was smoothed, primed and sprayed with high visibility enamel. Wet sanding concluded the process to produce a hard, smooth, wetting surface.

Six different surfaces, the common stern and each of the five bows, were completed in this manner. For each test the bow was aligned carefully and attached to the stern with four bolts to insure longitudinal rigidity. The completed model was gridded from the FP to Station 6 to facilitate flow visualization tests and relative bow motion observations. Cylindrical studs were placed on the hull at points 5% of the LPP back from the stem to induce turbulent flow conditions at all tested Reynolds numbers. Turbulent flow is necessary in testing since all flow around actual ships is turbulent. A single layer of plastic tape was placed around the joint between the two halves of each model to prevent flow disruption or leakage. Each model was then ballasted in still

water to a draft corresponding to 18 feet at ship scale at an even trim. Finally, dynamic ballasting procedures were followed to set the pitch gyradius at a nominal value of 0.25*LWL. This was done by setting the yaw gyradius with the bifilar suspension method. During the bifilar method, yaw gyradius is assumed to equal pitch gyradius. The model was then ready for testing.

4. EXPERIMENTAL TEST PROGRAM

The basic goals of the experimental program were to estimate the still water effective horse power (EHP) by measuring model resistance and speed, the seakeeping responses of pitch, heave, and relative vertical motion at Station 2, and the still water flow patterns around the bow for each model. The EHP and seakeeping tests were performed in the 380 foot towing tank of the U.S. Naval Academy Hydromechanics Laboratory (NAHL). The International Towing Tank Conference (ITTC) description of this facility is shown in Figure 4-1. For all tests, the dynamometer restrained the model in surge, sway, roll, and yaw. The towing point was held constant for all models at a point 2.2 inches aft of amidships and 1 inch below the DWL. Figure 4-2 shows Bow 5 attached to the dynamometer and the towing carriage. It also shows the box structure used to increase longitudinal rigidity. The depth of the fresh water for all tests was sixteen feet. Blockage effects were not a problem in the tests, since the blockage area ratio was less than 0.134% (with less than 0.5% considered acceptable).

The still water EHP tests covered a range of model speeds from 0.8 to 4.8 feet per second (ship speeds 3 to 18 kts), at intervals of 0.2 fps. Before testing for each model, the

INTERNATIONAL TOWING TANK CONFERENCE CATALOGUE OF FACILITIES

TOWING TANKS, SEAKEEPING AND MANOEUVRING BASINS

U. S. NAVAL ACADEMY HYDROMECHANICS LABORATORY — U.S.A.
ANNAPOLIS, MARYLAND 21402
TELEPHONE: (301) 267-3361

128m HIGH PERFORMANCE TOWING TANK (1979)

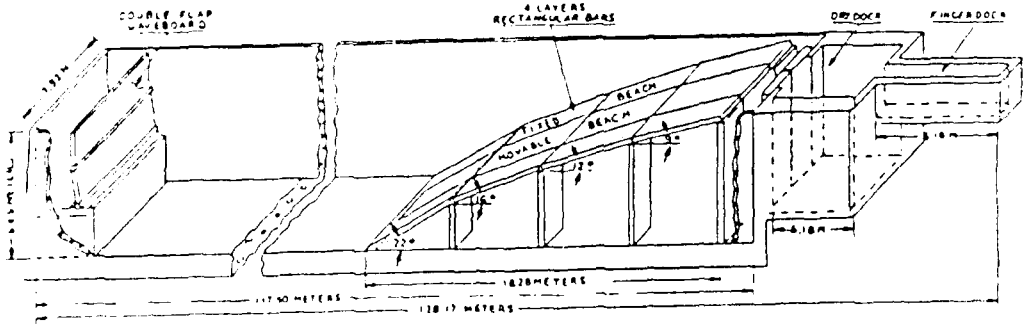

380 FOOT TANK AND WAVEMAKER

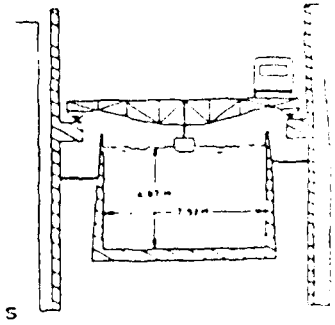

FIGURE A-1 IITC Description of the U.S. Naval Academy's 380 Foot Towing Tank

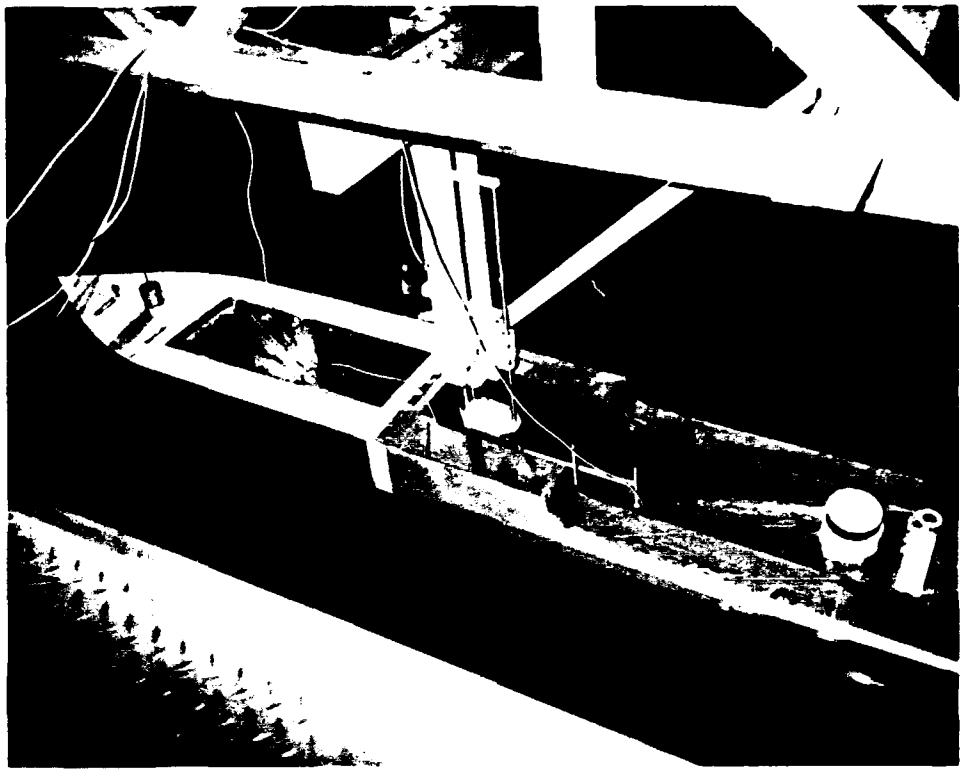

Figure 4-2, Model attachment to the 380' Tank Powered Carriage. Notice the dynamometry and the wooden box for longitudinal rigidity.

variable reluctance force block was calibrated. For each run, model speed and resistance were recorded and analyzed. Speed induced sinkage and trim in still water were measured and converted to vertical movements at the forward and after perpendiculars. Between each test run, a sufficient time was allowed for generated waves to dissipate, and the transducers rezeroed as necessary. Repeat speed runs were done to confirm validity of the data. Video tapes were made of all still water runs.

Seakeeping responses of pitch, heave, relative bow motion at Station 2, and resistance in waves were measured for each model in long crested, regular head seas. The nominal wave slope for the tests was 1/60. The wave frequencies ranged from those low enough to produce asymptotic limits of response to those high enough to produce near zero responses in pitch and heave. Extra runs were done near the frequencies of maximum response to establish the correct shape of the peak. Regular sea tests enabled the data at a tested speed to be summarized in the form of response amplitude operators (RAO's) so that ship response statistics in any desired sea state conditions, specified by modal frequency and significant wave height (SWH), could be computed assuming the applicability of the principle of linear superposition. Seakeeping tests were run at two discrete model speeds, 2.67 and 4.01 fps (10 and 15 kts ship speed). These speeds corresponded to those called out in the seakeeping requirements section of the Top Level

Requirements (TLR) for T-AGS OCEAN (ICE). The TLR requirements specify that the ship be able to maintain 15 knots at all headings in an 8' SWH, and 10 knots in a 12' SWH [10]. In addition, tests were done to estimate the natural pitch and heave frequencies by artificially inducing a response at zero speed in still water.

Before each regular wave model test, the transducers for heave (sinkage), pitch (trim), and resistance were calibrated. Model speed, encountered wave height (measured by a sonic probe), total resistance, pitch (trim) angle, and heave (sinkage at the bow point) were recorded for each run. Each model run was delayed until the generated waves reached the carriage start point, and recorded data were only used during the interval of steady state speed and encountered wave height. After each run, a sufficient amount of time was allowed for the generated wave systems to dissipate. All transducers were rezeroed as necessary. Video tapes were made of each run to observe deck wetness problems and relative bow motion at Station 2.

Flow visualization tests were conducted in the 120' towing tank of the NAHL using the powered carriage. The ITTC description of this tank is shown in Figure 4-3. Before each model was tested, yarn tufts were cut and affixed to the model at all waterline and station grid intersections below the DWL and back to Station 6 (of 20). The consistent tuft size was chosen so that they provide the most accurate picture of the

INTERNATIONAL TOWING TANK CONFERENCE CATALOGUE OF FACILITIES

TOWING TANKS, SEAKEEPING AND MANOEUVRING BASINS

U. S. NAVAL ACADEMY HYDROMECHANICS LABORATORY — U.S.A.
ANNAPOLIS, MARYLAND 21402
TELEPHONE: (301) 267-3361

36.6 m TOWING TANK (1976)

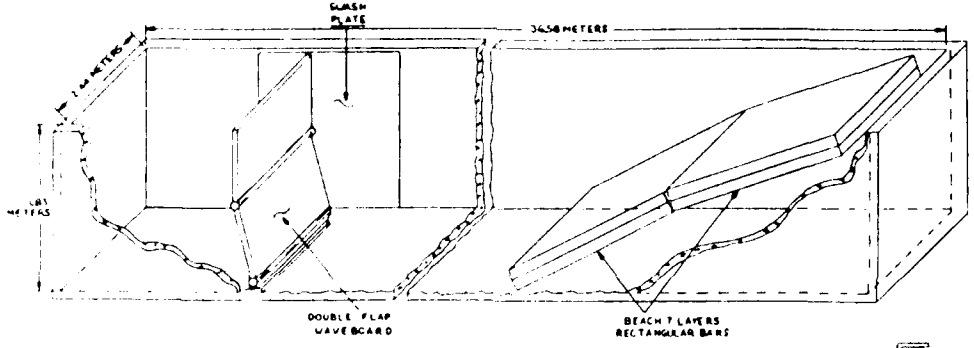

120 FOOT TANK AND WAVEMAKER SYSTEM

U.S. NAVAL ACADEMY

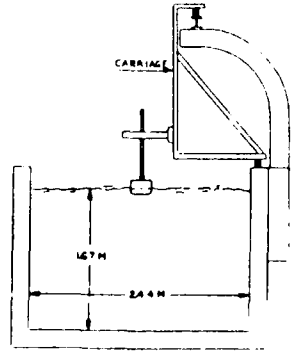

FIGURE 4-3, ITTC Description of the U.S. Naval Academy's 120 Foot Towing Tank

flow pattern in which they were placed. The 1.25 inch long, three-strand tufts were attached to the hull by a dollop of rubber cement. The model with tufts attached was allowed to soak for several hours before the flow visualization tests were run. These tufts were NOT present during the EHP and seakeeping tests. The 120' tank was chosen because the easily accessible windows along a portion of its length allowed easy video taping of the tufts. Blockage effects were not considered relevant since flow near the hull was the measurement of interest at very low speeds. For the same reason, no transducers for drag or motions were necessary.

Tests were run at model speeds corresponding to 5, 7.5, 10, 12.5, and 15 knots ship speeds. The forebody from the stem back to Station 6 was video taped for each run. Figure 4-4 shows an actual flow visualization test run in the 120' tank. Later, clear plastic overlays with a profile view of the forebody showing stations and waterlines scaled using FASTSHIP to match the model gridding as it appeared on the television monitor were used to record the tuft flow directions for each model at each test speed from the video tapes. The flow directions were then traced onto a similar profile view of the model on paper for qualitative analysis and comparison.

All raw experimental data from the still water, regular wave, and flow visualization tests are summarized in a separate report for general use [11].

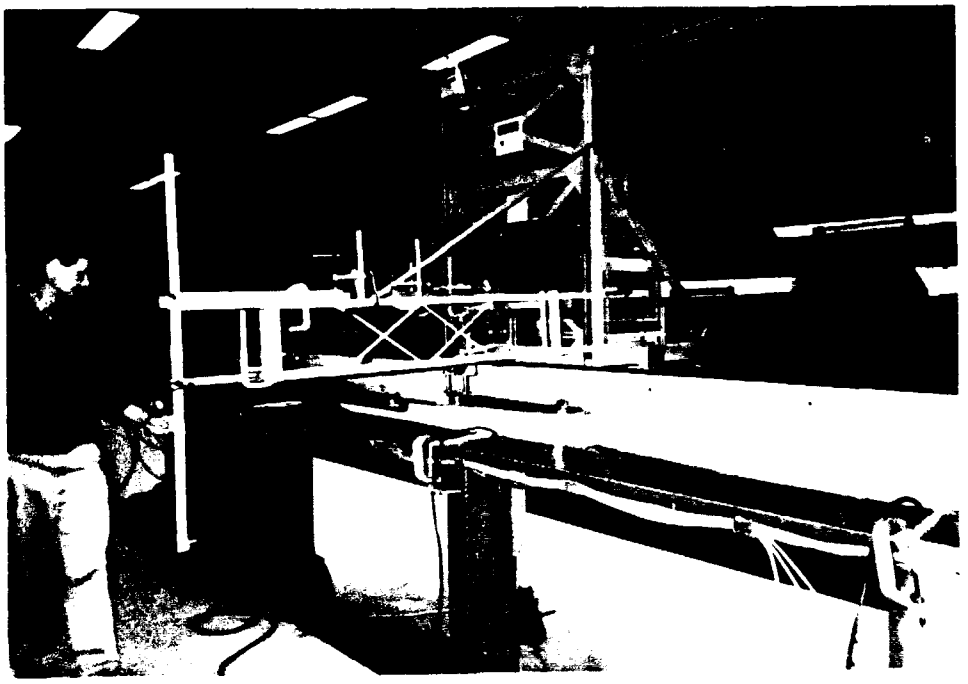

Figure 4-4, Model during Flow Visualization tests in the 120' Tank. Notice the video camera setup and the tank observation windows.

5. STILL WATER POWERING RESULTS

Values of total model resistance (lbs) and corresponding model velocity (fps) were obtained for each test run. The temperature of the fresh water in the 380' tow tank was also measured and recorded. A value for C_{Tm}, the model total resistance coefficient was derived from the total model resistance as follows:

$$C_{Tm} = \frac{R_{Tm}}{\frac{1}{2}\rho_m S_m V_m^2} \qquad (4)$$

where R_{Tm}, ρ_m, S_m, and V_m are total model resistance, tank water density, model wetted surface area, and model velocity respectively. Values of C_{Tm} based on measured data were plotted against V_m for each model. The author then created faired C_{Tm} curves based on his interpretation of the plotted data. Using the faired model C_{Tm} data, the Froude resistance expansion [12] was used to calculate values of total ship resistance at corresponding ship speeds. The ITTC 1957 formulation for C_F and a correlation allowance, C_A, of 0.0004 were used throughout this project for both model and ship. The residuary resistance coefficient, C_R was calculated by subtracting C_{Fm} from C_{Tm} at each model speed. A comparison plot of C_R for all five series members versus the

nondimensional Froude number ($F_n = V/(gLWL)^{1/2}$) is shown as Figure 5-1. This plot applies to both model and ship scale hulls for geometrically similar shapes. At very low speeds, C_R becomes constant since only form drag exists (i.e., no wavemaking occurs). At these speeds, it can be observed that no laminar flow problems (see Chapter 3) were present in the tests. Above a Froude number of about 0.125, wavemaking effects become significant and the curve begins to rise. Above a F_n of 0.25, the curve rises sharply. The primary function of this set of curves is to show the similarity in curve shapes. Systematic variations of a parent hull should have similar resistance curves, and these do, with a consistent hollow ($F_n \approx 0.125$), followed by a hump ($F_n \approx 0.2$), and then the sharp rise.

Total ship resistance was converted to effective horsepower, as a function of ship speed for final comparison. EHP represents the power that would be required to tow the ship at a certain speed through calm water. It does not provide for losses associated with the propulsive system of the ship, and, in this case, does not include the resistance associated with appendages such as rudders, bilge keels, or bossings. Figure 5-2 compares the EHP curve for each of the five series bows, plotted against ship speed (V_s (kts)). These curves are much more smooth than the C_R curves, and it is apparent that the shape of the curves, as predicted, are very similar. EHP begins at zero and gradually increases with

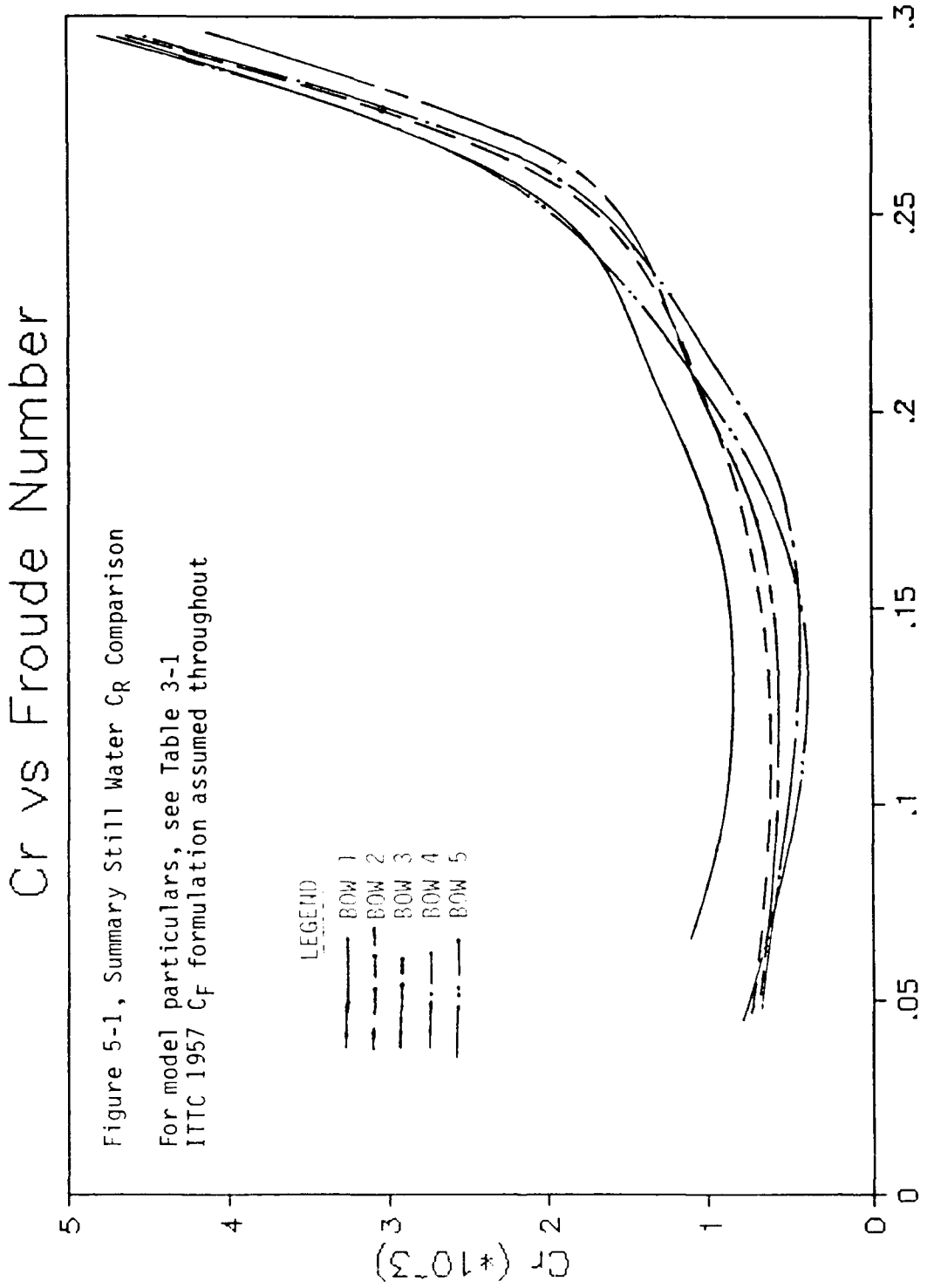
Cr vs Froude Number
Figure 5-1, Summary Still Water C_R Comparison
For model particulars, see Table 3-1
ITTC 1957 C_F formulation assumed throughout
LEGEND
BOW 1
BOW 2
BOW 3
BOW 4
BOW 5
Cr (*10^3)
Fn
0
1
2
3
4
5
0
.05
.1
.15
.2
.25
.3

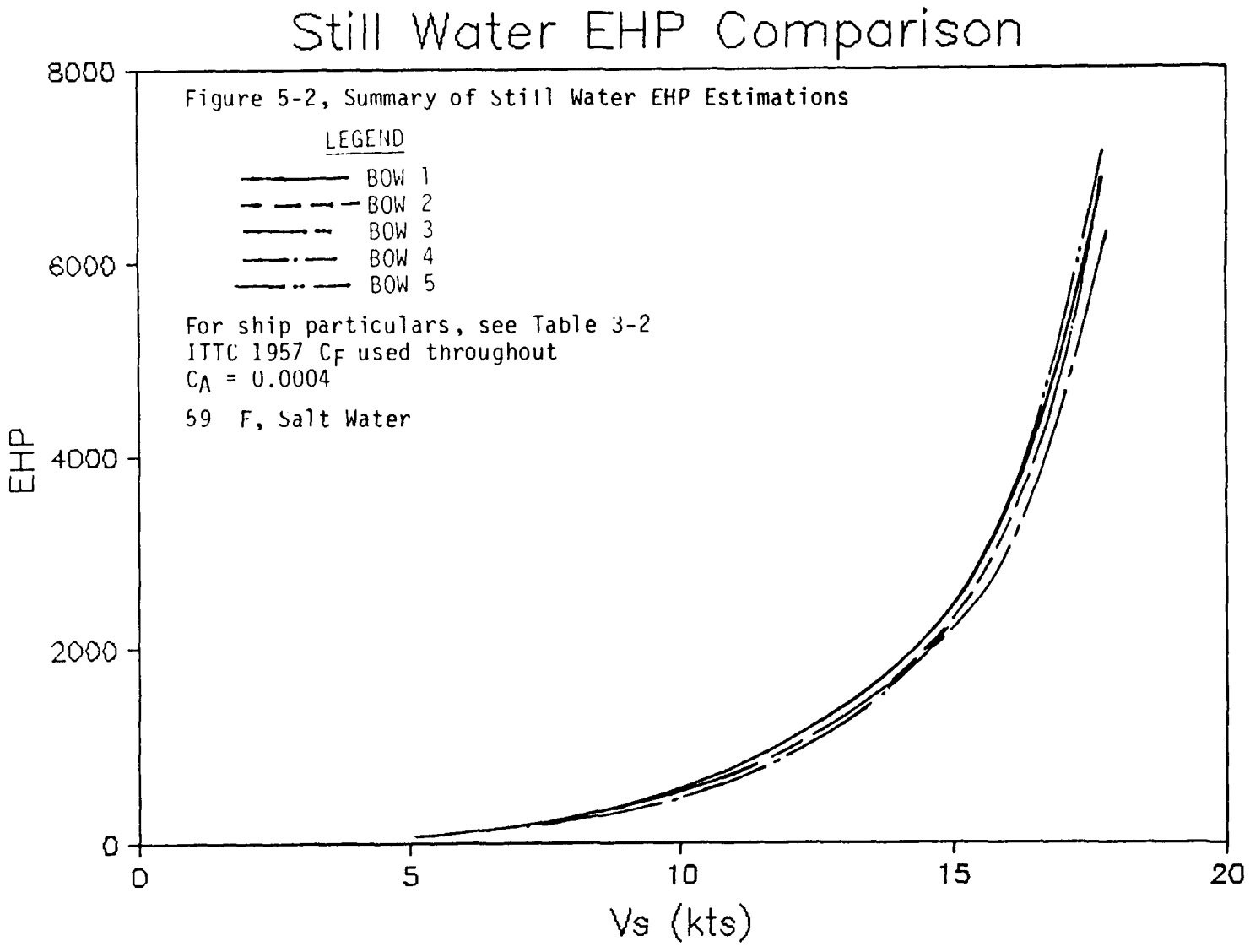
Still Water EHP Comparison
Figure 5-2, Summary of Still Water EHP Estimations
LEGEND
BOW 1
BOW 2
BOW 3
BOW 4
BOW 5
For ship particulars, see Table 3-2
ITTC 1957 C_F used throughout
C_A = 0.0004
59 F, Salt Water
EHP
8000
6000
4000
2000
0
0
5
10
15
20
Vs (kts)

ship speed. The slope of the curve also increases until EHP is rising extremely quickly at speeds above 15 knots. At the lower speeds, no readily apparent trend in the relative values of EHP is discernible. At higher speeds, Bow 5 had the highest EHP, while Bow 3 had the lowest. This was expected since Bow 5, the fullest, should produce the largest bow wave system, and Bow 3, the finest, should produce the smallest.

Table 5-1, below, presents a quantitative comparison of the five bows at a nominal design speed of 15 kts. The percentages were calculated as follows:

$$[\%Difference]_x = \frac{EHP_x - EHP_1}{EHP_1} \times 100 \qquad (5)$$

Table 5-1

Full Scale Still Water Powering Comparison at Vs = 15 knots		
	EHP	% Difference from Baseline
Bow 1	2428	-----
Bow 2	2280	-6.1
Bow 3	2196	-9.5
Bow 4	2289	-5.7
Bow 5	2480	2.2

At 15 kts, Bow 3, the finest, has the lowest EHP, about 10% less than the parent. Bow 2 and Bow 4, although fuller than the baseline, have somewhat less of a difference while still

showing a power advantage. Bow 5, the fullest, is the only bow at this speed with an EHP higher than Bow 1, and its percent increase of just over 2% is fairly modest. The maximum drop of ten percent in Bow 3 is significant, but must be considered simultaneously with the knowledge that it falls on the boundary representing the lightest icebreaking capability in terms of the Shimansky parametric comparison shown earlier as Figure 3-10. Bows 2 and 4, although their percent differences are less significant, do fall more within the normal icebreaking range, as characterized by the Shimansky comparison. Most remarkably, Bow 5, the most ice-capable of the icebreakers, has a relatively low penalty in still water powering.

Finally, Figure 5-3 presents a different form of the open water ship resistance data. In it, a ratio of total ship resistance (lbs) to displacement (LTSW) is plotted against Froude Number for all five bows. This presentation serves to normalize the total resistance values for all hulls. Superimposed on the curves are the R_T/Δ values for other icebreakers. [13]. These other icebreakers include the WYTM 140, the WIND Class, the "R" Class, the B-AL, and the POLAR Class. The other ships have values which form curves similar in shape to those of the tested bows, and those of the "R" Class, the B-AL, and the POLAR Class in particular fall near the curves for the tested bows.

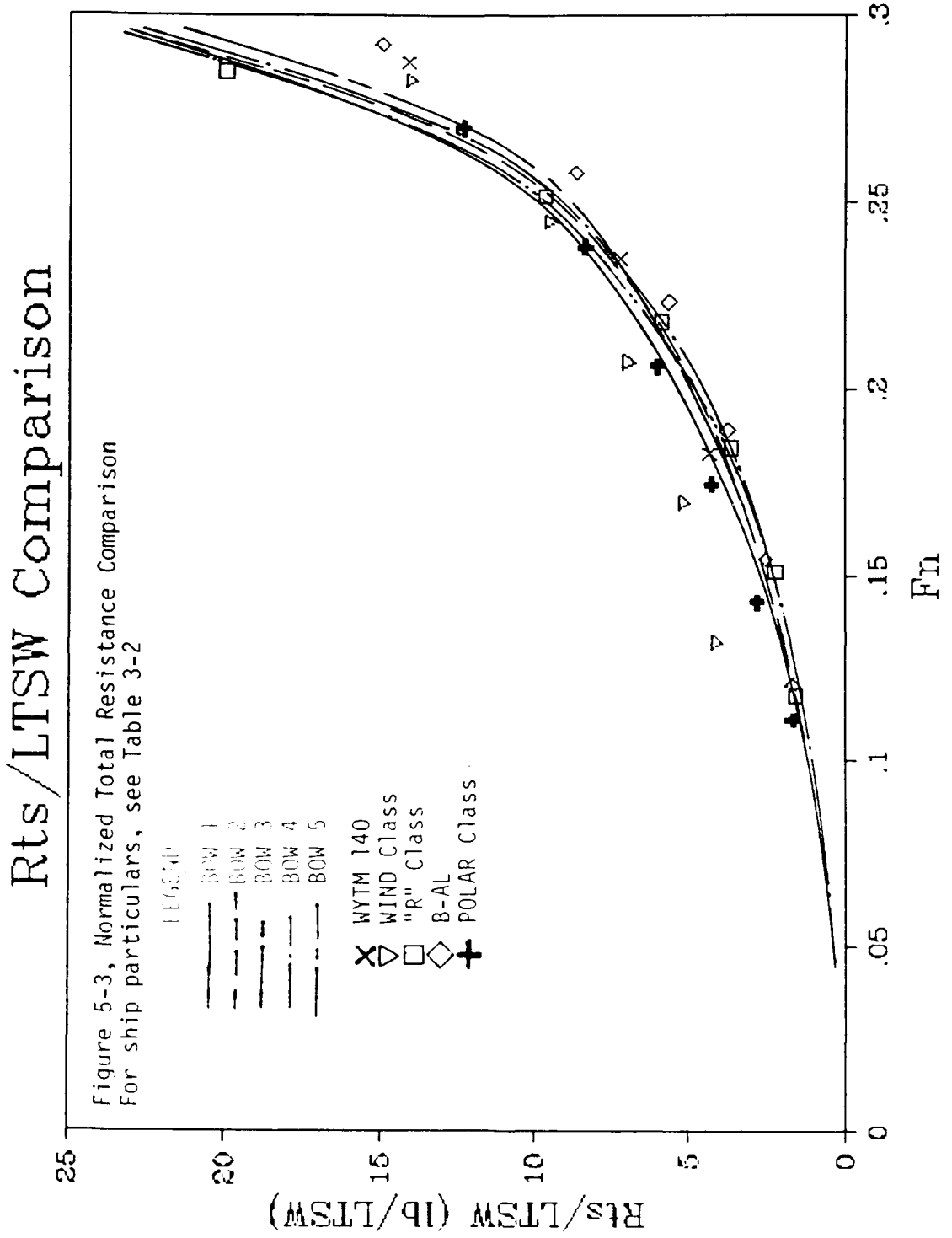
Rts/LTSW Comparison
Figure 5-3, Normalized Total Resistance Comparison
For ship particulars, see Table 3-2
BOW 1
BOW 2
BOW 3
BOW 4
BOW 5
WYTM 140
WIND Class
"R" Class
B-AL
POLAR Class
Rts/LTSW (lb/LTSW)
Fn
0
5
10
15
20
25
.05
.1
.15
.2
.25
.3

This comparison serves as a basic check on both the testing procedures and the validity of the choice of parent hull. Any unusual features in the test results as compared to operating icebreakers could have cast both into doubt.

6. SEAKEEPING RESPONSES

For each regular, head seas test run, transfer functions were obtained for pitch, heave, relative bow motion at Station 2, and added resistance in waves at two discrete speeds.* Model speeds corresponding to full scale ship speeds of 10 and 15 knots were chosen for the series models. Transfer functions (TF's) present the double amplitude of the response per unit wave height, and when squared become response amplitude operators (RAO's). Transfer functions were developed from the measured data and were used for fairing purposes.

Pitch transfer functions were in the form of double pitch amplitude (2θ in degrees) per unit wave height (Hw in inches). Heave transfer functions were in the dimensionless form of double heave amplitude (2Z) per unit wave height. Relative bow motion (RBM) at Station 2 was obtained by visual observation of the relative vertical motion between the water surface and the model gridding from each video taped test run*. The relative motion transfer function was developed after division by the encountered wave height. The added resistance in waves RAO was obtained by subtracting the faired

---

* Relative bow motions at Station 2 were not acquired for Bow 1 due to gridding problems above the design waterline. Relative bow motions and added resistance in waves were not analyzed for Bow 4 due to inconsistency of the acquired data.

still water resistance in pounds at the same model speed from the average total resistance in pounds of the model at each wave frequency in regular seas. These values were then divided by the square of the wave height in feet, as added resistance in waves is considered proportional to the square of the wave height [14]. Taking the square root of this RAO yields the transfer function in units of $((lbs)^{1/2}/(ft)$.

These model transfer functions were plotted versus model encounter frequency, and faired curves drawn. These curves represent the author's best interpretation of the data and were created with the knowledge that models in a systematic series should have curves with somewhat similar response characteristics. Hand drawn curves were chosen over computer calculated curves because they do allow intuitive interpretation. The faired transfer function curves are presented for comparison between bows in the following figures: Figures 6-1 and 6-2, Pitch; Figures 6-3 and 6-4, Heave; Figures 6-5 and 6-6, Relative Bow Motion (RBM) at Station 2; and Figures 6-7 and 6-8, Added Resistance in Waves. For each response, the first of the two figures applies to the lower model speed, while the second applies to the higher speed.

In the final step of the response in head seas data analysis, the model transfer functions were used to predict the significant double amplitude responses of pitch, heave, and relative motion at Station 2 in irregular, head seas.

Added EHP in irregular waves was not predicted. Added resistance values, once calculated after the testing, did not appear to drop to any logical asymptotic limit within the tested range of wave frequencies, as did the other three responses.

A computer program written in BASIC was used to combine and expand the transfer functions with sea spectra to response spectra in irregular, head seas at each corresponding ship speed (10 and 15 kts). A sample run output of this program is included as Appendix 6-1. Significant response double amplitudes** were calculated using the principle of linear superposition at the same seastates specified in the T-AGS OCEAN (ICE) TLR (SWH 12' at 10 kts, 8' at 15 kts). The irregular wave systems were defined using the ITTC one-parameter wave spectrum equation. The significant double amplitude responses are presented within tables later in this chapter.

As stated in Chapter 4, the natural response frequencies for pitch and heave were obtained experimentally for the purpose of predicting the encounter frequencies at which maximum (resonant) responses should occur. As many distinct peak-to-peak periods as possible were measured from each natural response test. The highest and lowest values for each bow in pitch and heave were dropped, and the remaining periods

---

** "Significant", in this context, means the average of the one-third highest responses.

were averaged. The natural frequency of motion was calculated from this average peak-to-peak period. These natural frequencies are presented below in Table 6-1. Note that the purpose of these natural frequency tests was to confirm the validity of the regular wave test results. These frequencies are not in exact agreement with the experimentally obtained resonant frequencies, but are close and support the validity of the tests.

Table 6-1
Natural Frequencies of Motion (Hz), Pitch and Heave

	Pitch	Heave
Bow 1	1.012	1.070
Bow 2	1.004	1.082
Bow 3	0.982	1.092
Bow 4	0.848	1.071
Bow 5	0.966	1.064

Figure 6-1 and 6-2 show the model pitch transfer functions at 2.67 and 4.01 fps, respectively. In both cases, the pitch responses follow the wave slope at near zero encounter frequencies, rise to a maximum at resonance, and then decline again to zero at high frequencies. At both speeds, Bow 1 and Bow 2 have the highest peak responses, Bow 3 and Bow 4 have similar but lower peak responses, and Bow 5 has the lowest peak response. Table 6-2a and 6-2b compare the expanded significant double amplitude pitch responses for each bow at 10 and 15 kts in the corresponding seastates,

Pitch Transfer Function (Vm = 2.67 fps)

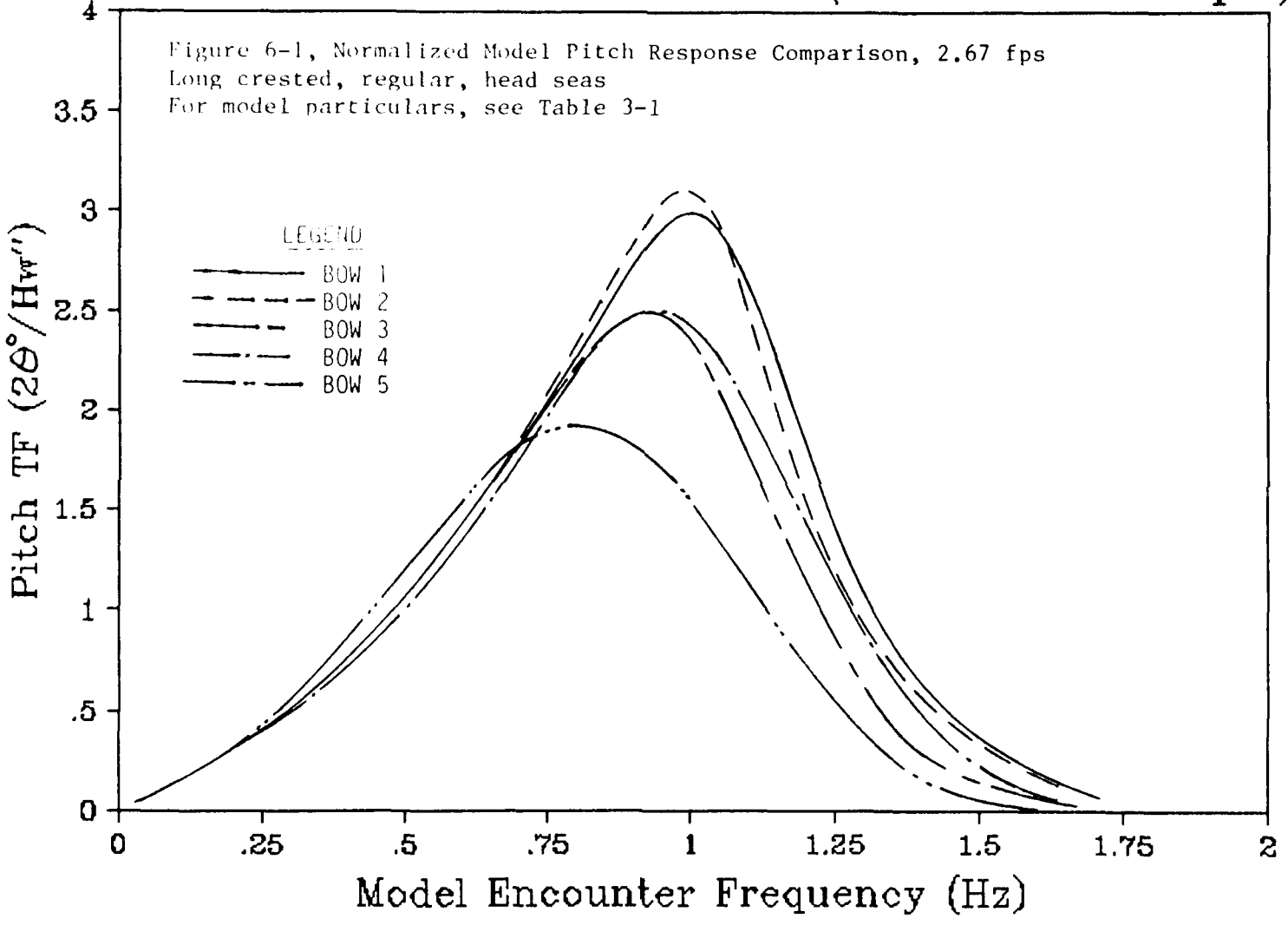

Pitch Transfer Function (Vm = 4.01 fps)

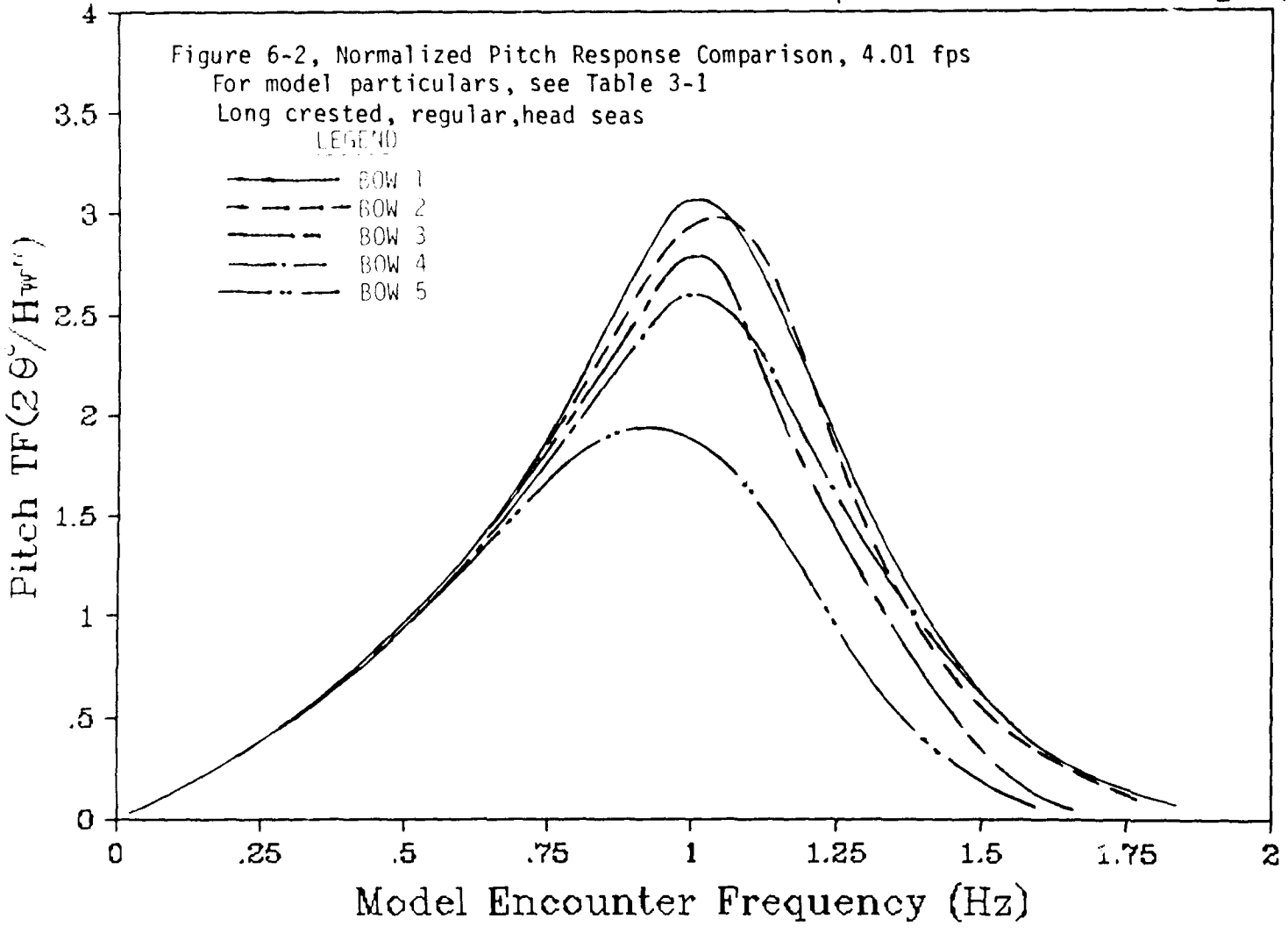

respectively. $S_{1/3}$ is the average of the one-third highest responses the ship would experience, while $S_{1/10}$ is the average of the one-tenth highest responses. In the last column are the percent differences between the significant responses for each bow from the baseline (Bow 1).

$$[\%Difference] = \frac{(S_{1/3})_x - (S_{1/3})_1}{(S_{1/3})_1} \times 100 \qquad (6)$$

Table 6-2a
Significant Pitch Responses (10 kts)
NATO Seastate 5 (12'SWH, 25.5 kt Wind)

	$S_{1/3}$ (°)	$S_{1/10}$ (°)	% Diff
Bow 1	7.21	9.19	----
Bow 2	7.22	9.21	0.2
Bow 3	6.08	7.75	-15.7
Bow 4	6.26	7.98	-13.2
Bow 5	4.66	5.95	-35.3

Table 6-2b
Significant Pitch Responses (15 kts)
NATO Seastate 4 (8' SWH, 20.8 kt Wind)

	$S_{1/3}$ (°)	$S_{1/10}$ (°)	% Diff
Bow 1	3.36	4.29	----
Bow 2	3.29	4.19	-2.1
Bow 3	2.78	3.55	-17.3
Bow 4	2.88	3.67	-14.3
Bow 5	1.97	2.51	-41.4

At each speed and seastate, Bow 5 has the lowest pitch response by far. One should note that although the transfer functions at 4.01 fps are higher than those at 2.67 fps, the lower significant wave height specified for the higher ship speed results in noticeable decreases in pitch response.

Figures 6-3 and 6-4 present the model heave transfer functions for 2.67 and 4.01 fps, respectively. At both speeds, the normalized response in very low frequency waves begins at one. The normalized responses gradually begin to decline towards zero at high frequencies, with a resonant peak at the natural frequency. The heave response follows the pattern of the pitch response, with Bow 1 and Bow 2 being the highest, Bows 3 and 4 at midrange, and Bow 5 being the lowest. At both speeds, Bow 5 experiences almost no resonant peak in its heave response - quite a desirable characteristic. As for pitch, Tables 6-3a and 6-3b present the expanded double amplitude heave responses for each bow at 10 and 15 kts in the corresponding seastates, respectively.

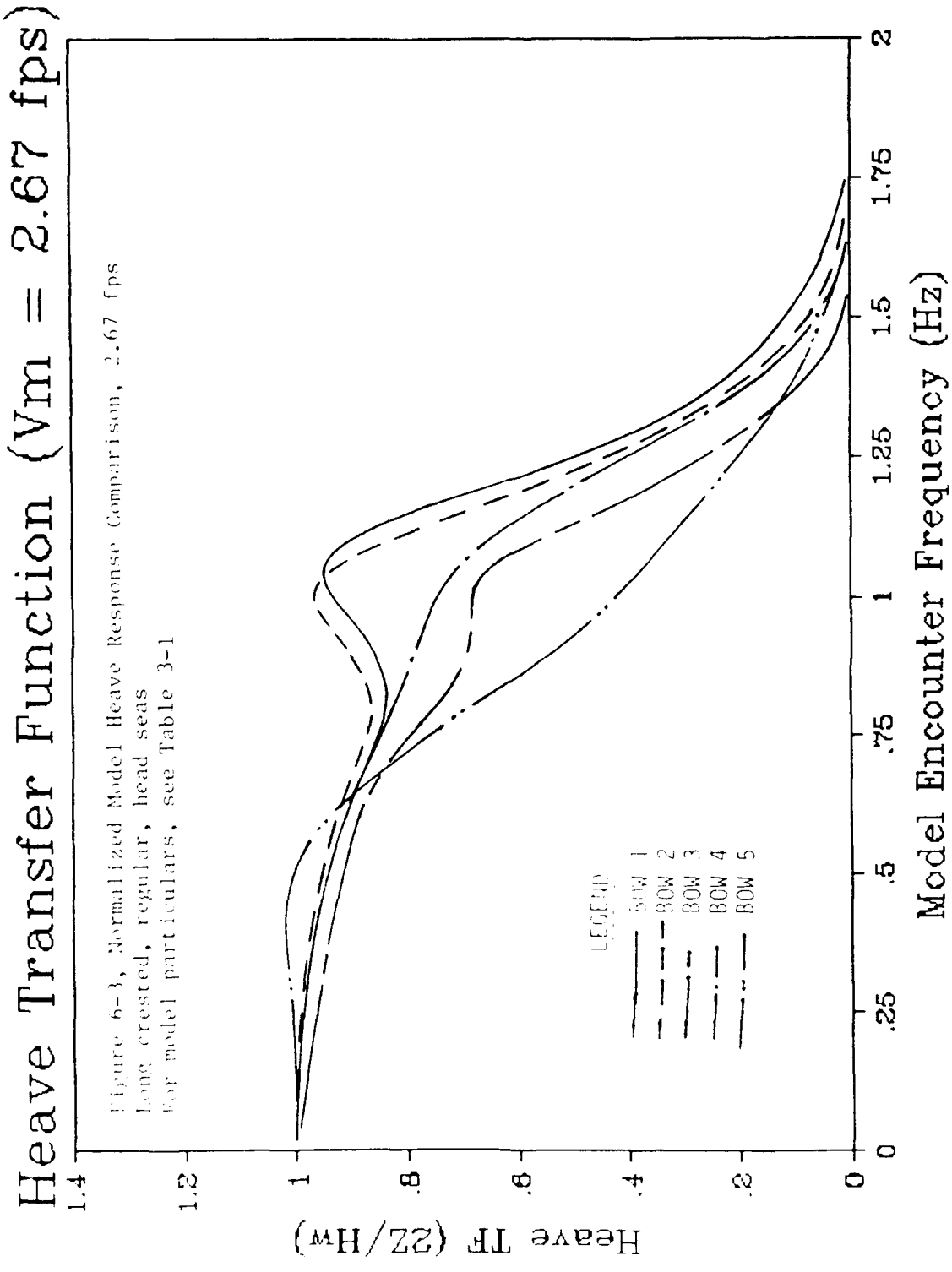
Heave Transfer Function (Vm = 2.67 fps)
Figure 6-3, Normalized Model Heave Response Comparison, 2.67 fps
Long crested, regular, head seas
For model particulars, see Table 3-1
Heave TF (ΔZ/Hw)
Model Encounter Frequency (Hz)
LEGEND
BOW 1
BOW 2
BOW 3
BOW 4
BOW 5
0
.2
.4
.6
.8
1
1.2
1.4
0
.25
.5
.75
1
1.25
1.5
1.75
2

Heave Transfer Function (Vm = 4.01 fps)

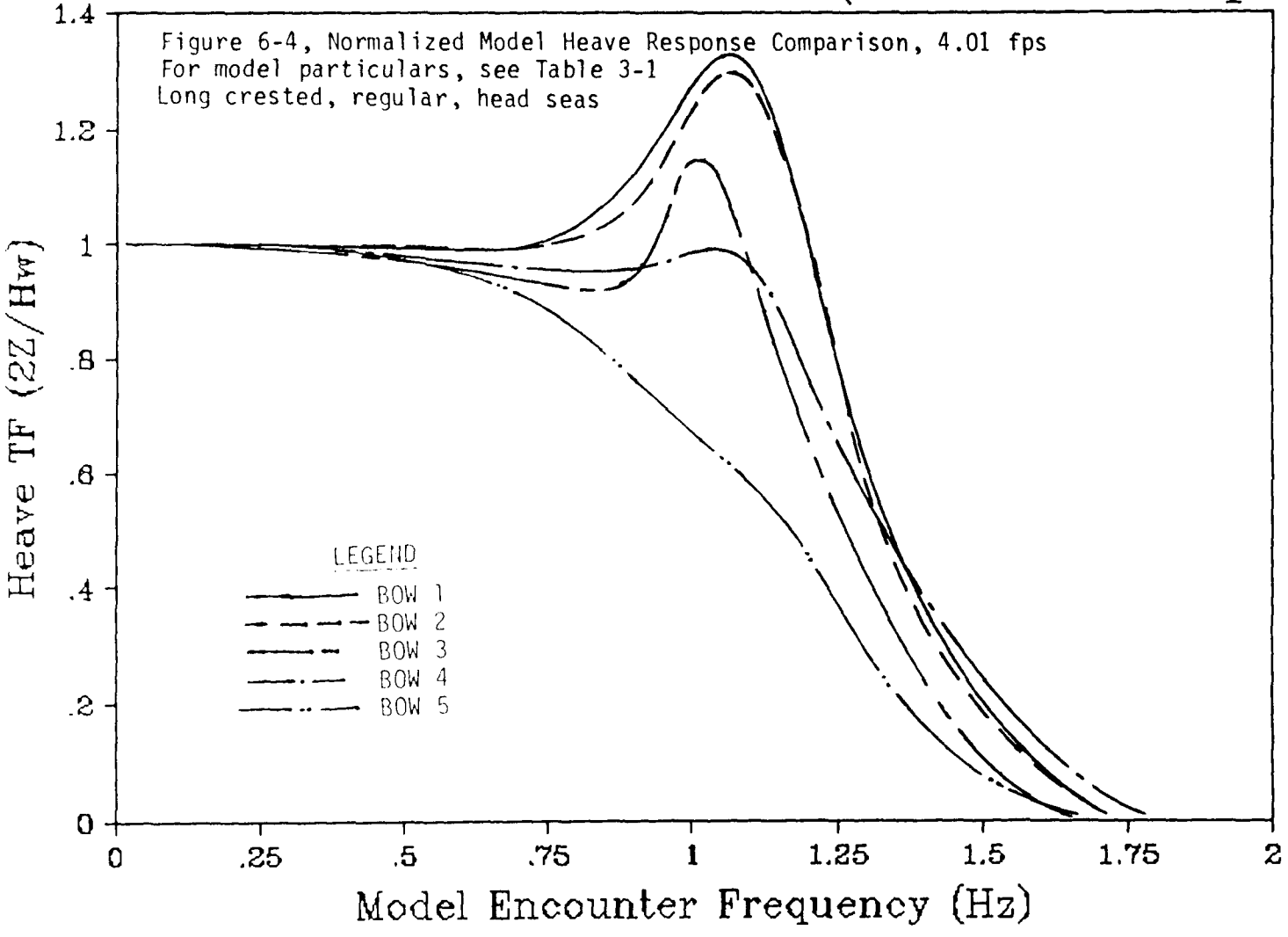

Table 6-3a
Significant Heave Responses (10 kts)
NATO Seastate 5 (12'SWH, 25.5 kt wind)

	$S_{1/3}$ (ft)	$S_{1/10}$ (ft)	% Diff
Bow 1	8.36	10.66	----
Bow 2	8.37	10.67	0.1
Bow 3	6.60	8.41	-21.1
Bow 4	7.42	9.46	-11.3
Bow 5	5.60	7.14	-33.0

Table 6-3b
Significant Heave Responses (15 kts)
NATO Seastate 4 (8' SWH, 20.8 kt wind)

	$S_{1/3}$ (ft)	$S_{1/10}$ (ft)	% Diff
Bow 1	4.78	6.10	----
Bow 2	4.65	5.92	-2.8
Bow 3	3.70	4.72	-22.6
Bow 4	3.88	4.94	-18.9
Bow 5	2.47	3.15	-48.3

As with pitch, Bows 1 and 2 experienced the highest responses, while Bow 5 experienced the lowest responses with a maximum percent difference of almost 50%.

Figures 6-5 and 6-6 present the relative bow motion at Station 2 transfer functions at 2.67 and 4.01 fps, respectively. There are no data for either Bow 1 or Bow 4 as explained in the earlier footnote. This does not seriously hamper analysis, as RBM response should be strongly correlated to pitch and heave responses and their relative phases. Since

Relative Bow Motion @STA2 TF (Vm=2.67 fps)

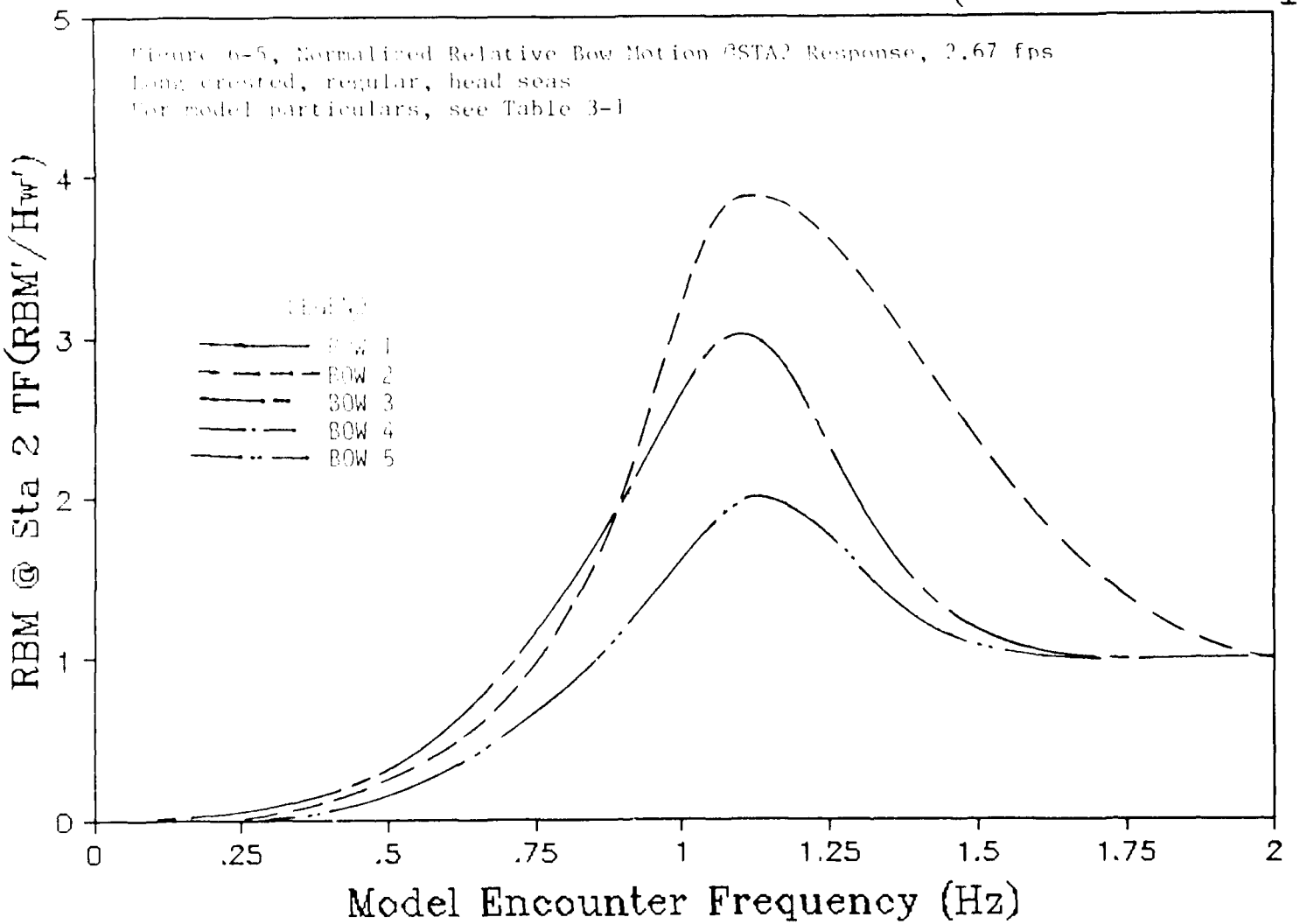

Relative Bow Motion @STA2 TF (Vm=4.01 fps)

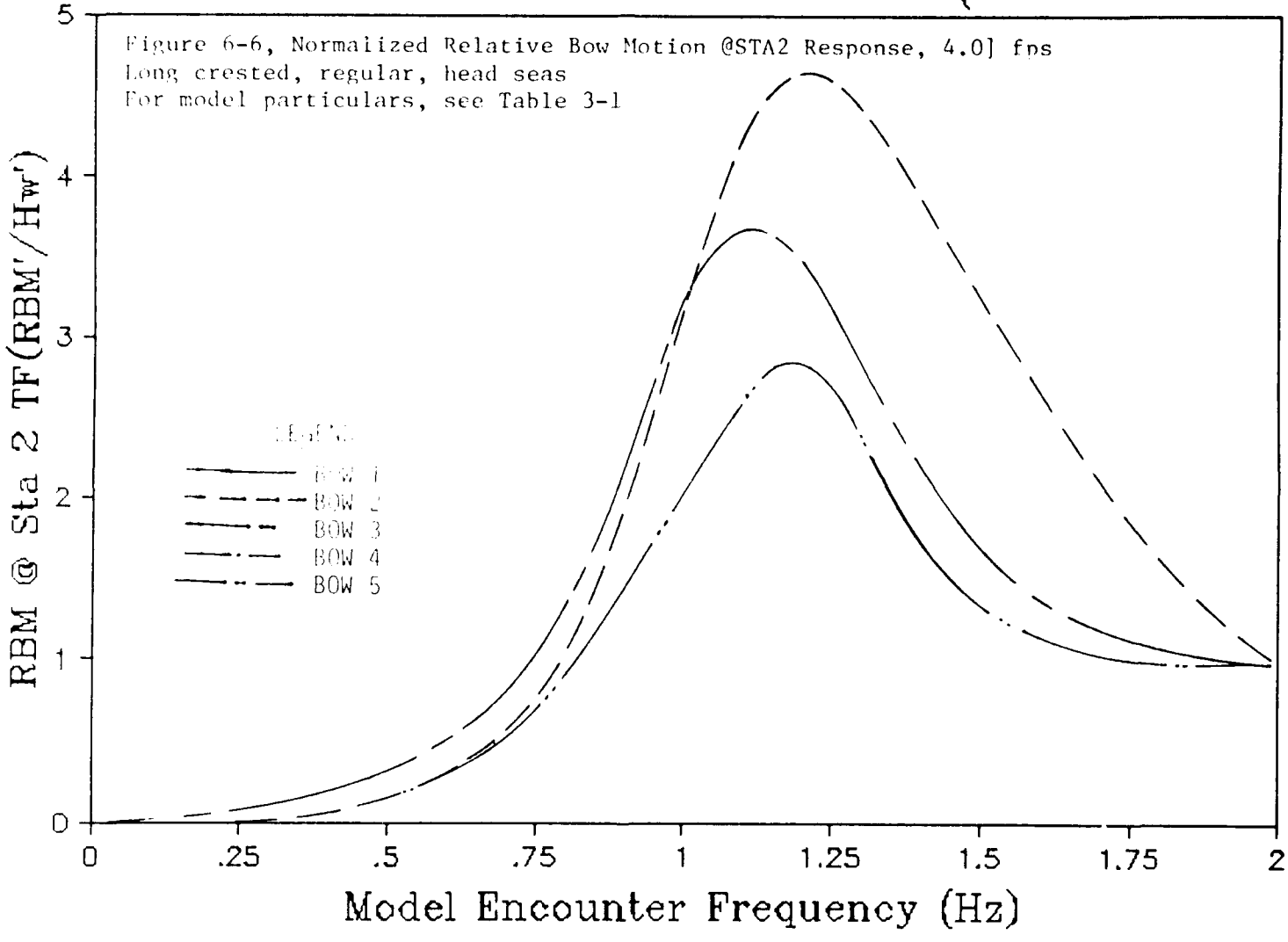

the previous trends have shown Bow 1 to be near Bow 2, and Bow 4 to be near Bow 3, the same is assumed true for RBM. Visual observation of video taped regular waves tests of all the models supports the validity of this assumption. The RBM curves begin at zero at low encounter frequencies, reach a resonant peak, and approach a value of one asymptotically as the high frequency, short wavelength waves encounter the hull. Tables 6-4a and 6-4b compare the significant relative bow motion responses at Station 2 at 10 and 15 kts respectively. The percent difference in this table is with respect to Bow 2.

Table 6-4a
Significant RBM @Sta2 Responses (10 kts)
NATO Seastate 5 (12'SWH, 25.5 kt wind)

	$S_{1/3}$ (ft)	$S_{1/10}$ (ft)	% Diff
Bow 1	N/O	N/O	N/O
Bow 2	29.2	37.2	----
Bow 3	22.6	28.8	-22.6
Bow 4	N/O	N/O	N/O
Bow 5	15.2	19.4	-48.0

Table 6-4b
Significant RBM @Sta2 Responses (15 kts)
NATO Seastate 4 (8' SWH, 20.8 kt wind)

	$S_{1/3}$ (ft)	$S_{1/10}$ (ft)	% Diff
Bow 1	N/O	N/O	N/O
Bow 2	22.6	28.9	----
Bow 3	16.4	20.9	-27.7
Bow 4	N/O	N/O	N/O
Bow 5	12.8	16.3	-43.4

When analyzing relative bow motion data, the importance of the response magnitudes depends primarily upon the depth (vertical distance from keel to deck at edge) of the ship at the station of interest. On T-AGS OCEAN (ICE) and all four variants, the depth, H, at Station 2 is 38 feet. If the RBM reaches a value greater than H, then it is possible that the forecastle may either plunge into the water or that the forefoot may emerge. Forefoot emergence would especially be dangerous on a ship with a bow sonar dome, possibly causing great damage to the sonar. At the two design conditions set in the TLR, the only significant probability of either deck plunging or forefoot emergence would be on Bow 2 (and presumably Bow 1) at 10 kts in seastate 5 (12' SWH). With a $S_{1/10}$ response amplitude of 37.2 on Bow 2, the chances of RBM being larger than H are greater than for any other combination tested.

The video taped test runs were also used to observe deck wetness trends during regular wave testing. Deck wetness can be a serious hindrance to the efficient performance of a ship in open water. None of the models experienced any significant deck wetness problems at the low test speed, 2.67 fps. At 4.01 fps, however, deck wetness was much more common. Although no formal analysis was done concerning deck wetness, general observation revealed that the finer bows, Bows 1, 2, and 3, had a lower frequency of occurrence than did Bows 4 or 5. At first this observation seems to make little sense, as

Bows 4 and 5 have had lower seakeeping responses than the parent. However, when one considers the trend in LCB among the hulls, the answer becomes clear. Because the displacements of Bows 4 and 5 are centered further forward (more capable in ice), they tend to drive through the waves more than do the others. Responses are still low, but wetness becomes a problem. This problem may be solved without losing the advantages gained in seakeeping, however. For instance, freeboard forward could be increased by adding a bulwark.

Perhaps a better method of improving deck dryness involves modifying the hard chine shown in the lines drawings above the design waterline. The original purpose of this chine was to allow some flare at the DWL amidships without increasing the maximum beam to an unreasonable level. This is not as much a concern near the forward perpendicular, as long as overall maximum beam is not increased. By observing the tapes, the author noticed that when the bow began to pitch downwards, the high flare served to push the rising water away from the model. At higher RBM's, the water reaches this chine and suddenly is free to move up the near vertical side of the model until it reaches the deck-at-edge and causes deck wetness. By maintaining as much flare as possible near the stem to the deck-at-edge (reducing the chine sharpness forward), deck wetness may be reduced significantly.

Figures 6-7 and 6-8 present a comparison of the model added resistance in waves transfer functions for 2.67 and 4.01

Added Resistance in Waves TF (Vm=2.67 fps)

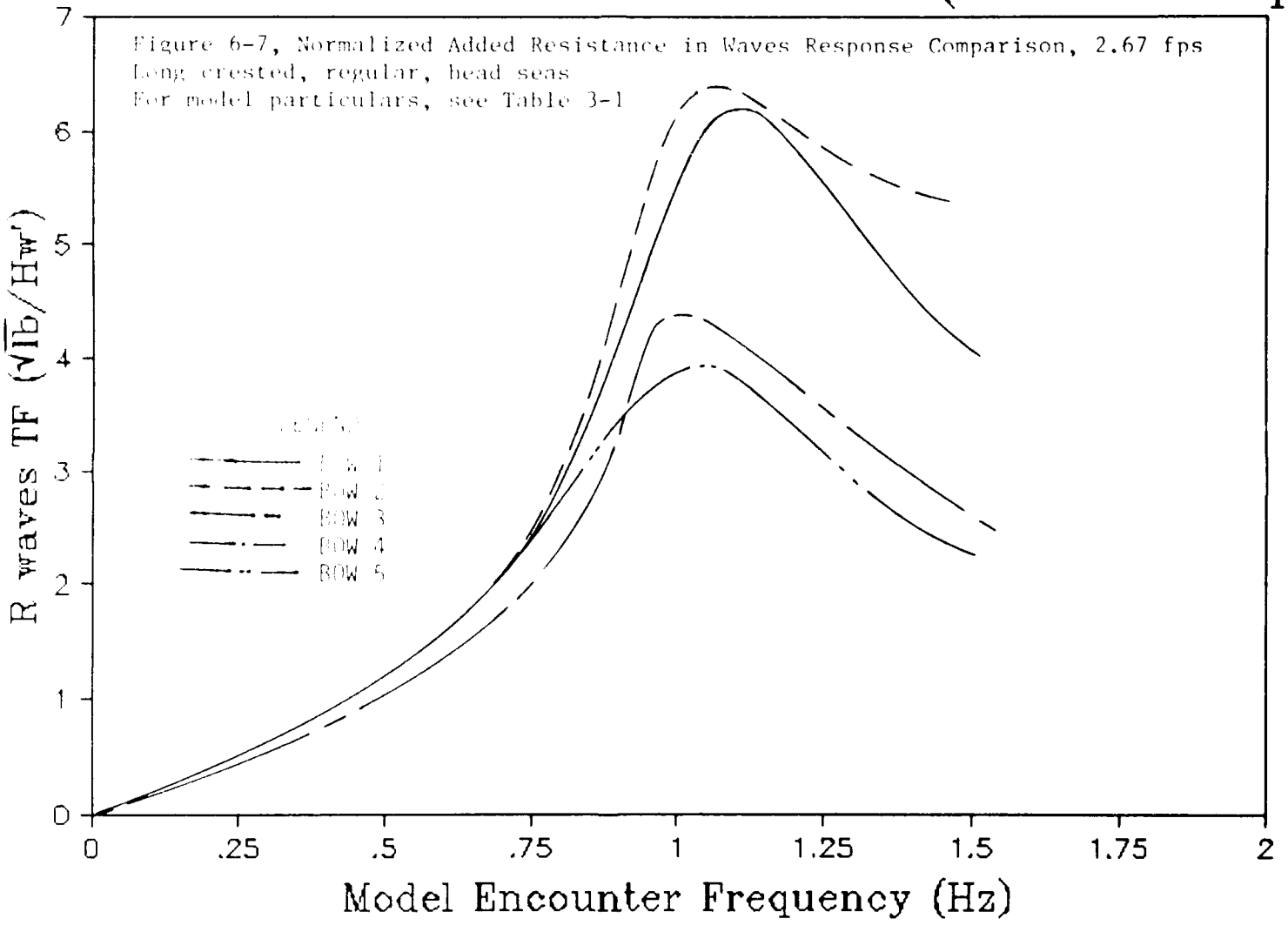

Added Resistance in Waves TF (Vm=4.01 fps)

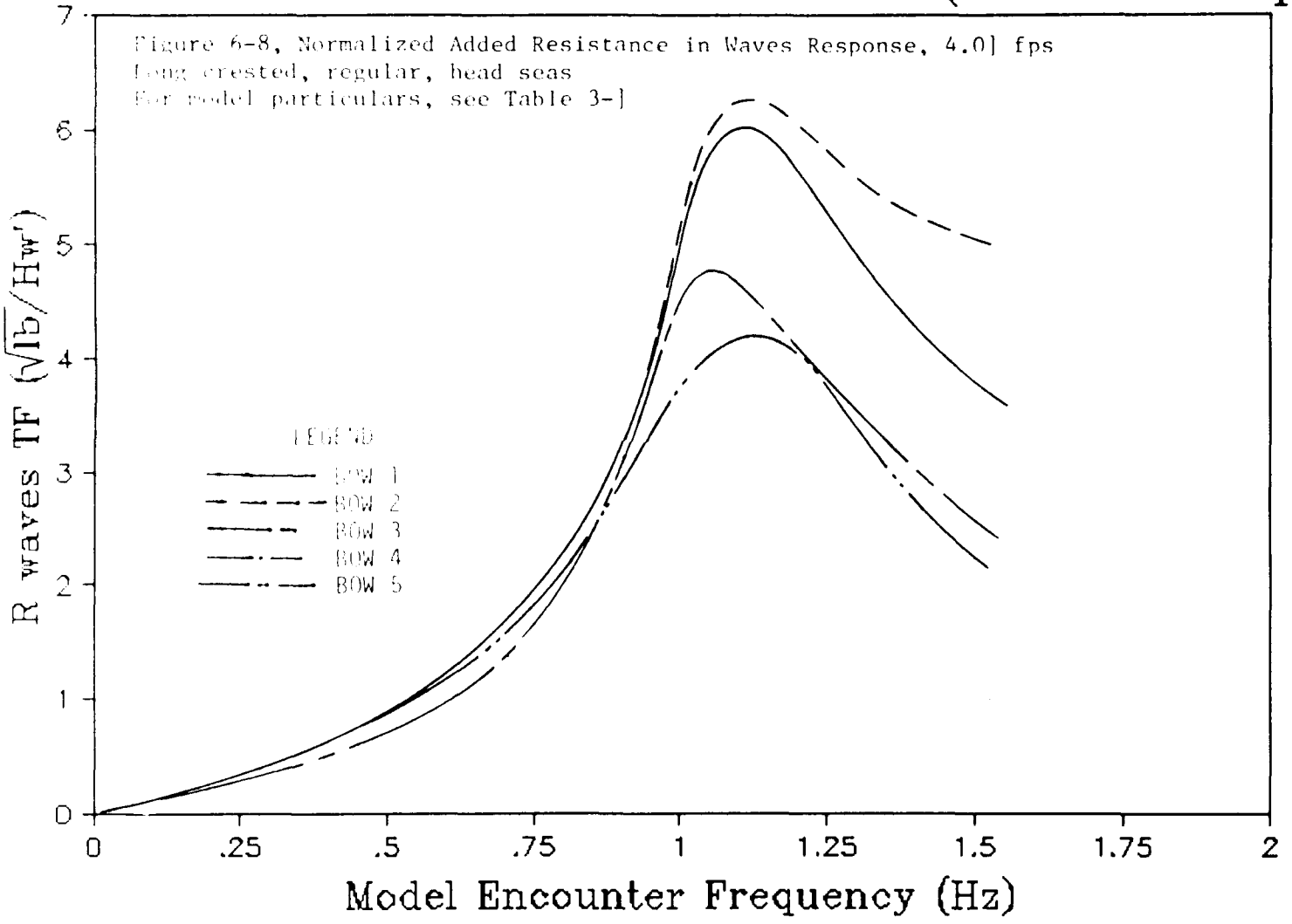

fps, respectively. There are no data for Bow 4 as discussed previously. The response curves begin at zero for low encounter frequencies, approach resonant response sharply, and then slowly decrease with increasing encounter frequency. Again, this slow decrease prevented the use of the model data for ship scale added resistance predictions. The transfer function curves follow the same trend seen in the earlier responses. This is logical, as added resistance in waves is almost completely a function of the pitch and heave responses [15]. Bow 1 has the highest added resistance due to waves, and Bow 5 has the lowest response.

During the testing, an interesting and possibly important side effect of the hull form was observed. The bottom of the transom sits just above the free surface when the ship is floating at the design draft without trim. This arrangement is chosen to prevent structural difficulties when backing in ice (the stern would also greatly increase the in-ice resistance while backing). Although not precisely measured, there is evidence (from observing the test runs in regular seas) that the stern would experience some slamming problems when moving in a seaway. The exact magnitude of this undesirable side effect is unknown.

In summary, the results reveal that as flare angle (β) and waterline angle (α) are increased, all four seakeeping responses analyzed - pitch, heave, RBM @Sta 2, and added resistance in waves - become better, i.e., decrease. The only

detrimental effect observed involved the disadvantage of increasing deck wetness, and a possible solution has been proposed by the author.

7. FLOW VISUALIZATION ANALYSIS

The mission requirements of the T-AGS OCEAN (ICE) necessitate installation and use of both wide beam and multi-beam, deep and shallow water, hydrographic sonars for the bottom mapping and survey function [16]. The TLR for the ship requires minimal flow interference with the sonar throughout the speed range of its operation. As described in Chapter 4, flow visualization tests were conducted to determine the effect of the systematic flare and waterline angle variations on the hydrodynamic flow in the area from the stem to the sonar. The proposed location of the sonar will be on the flat of bottom between Stations 5 and 6 (25 to 30% LPP aft FP).

The primary concern of interference lies with noise around the sonar windows, especially bubble sweepdown, and, at low speeds, ice flow near the sonar. The questions concerning bubble interference are particularly valid for ice-capable ships, since many may feature ice lubrication systems having the purpose of reducing the total ship resistance by producing bubbles near the bow which will move over the hull while traveling in ice-congested areas.

Flow streamlines were traced over profile views of each tested bow at each of five speeds by analyzing the patterns of the tuft flow directions. After review of the ship's

operational characteristics, it was decided to compare the streamlines at two of the tested speeds, 5 and 12.5 kts ship speed, for each bow. 5 knots was chosen since the sonar would presumably be operating while moving at the lower end of the speed scale to minimize normal hull and propulsion noise (and certainly if the operational area were ice covered, see Figure 2-1). 12.5 knots corresponded with the high end of the sonar operating range as stated in the TLR. Additionally, only the results for Bow 3 and Bow 5 are presented in the main body of this report, as they define the full range of bow angles. The pattern of change from Bow 3 to Bow 5 for each speed is orderly and logical, so that presenting both ends of the series makes good sense. The streamlines for all five bows at 5 and 12.5 knots ship speed are presented in Appendices 7-1 (a-e) and 7-2 (a-e). Figure 7-1 compares the flow streamlines for Bow 3 and Bow 5 at 5 kts ship speed, while Figure 7-2 makes the same comparison at 12.5 kts.

At 5 kts no noticeable surface wave was observed for any of the bows. In Bow 3, the streamlines tend to cross the buttock planes, rather than following them, so that there is some indication that the flow might possibly sweep underneath the hull near Stations 5 and 6. The effect does not appear to be a severe one, but may be of concern, since at the low speed, the chance of ice sweepdown would be of much greater relevance. In Bow 5, although the reason is not clear at this speed, flow follows the shape of the buttocks near Stations 5

Figure 7-1, Flow Streamline Comparison

BOW 3 at 5.0 KNOTS

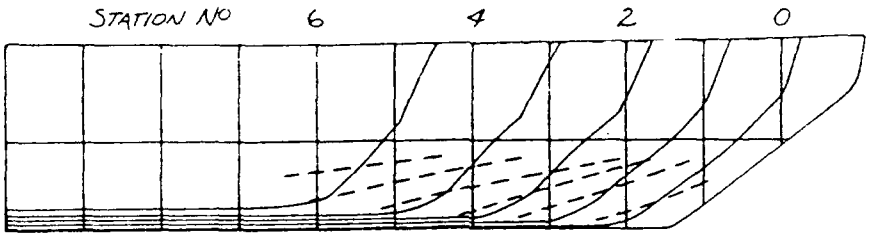

NOTES:
(1) Proposed bottom mapping sonar system location: between Stations 5&6
(2) No noticeable surface wave at this low speed

BOW 5 at 5.0 KNOTS

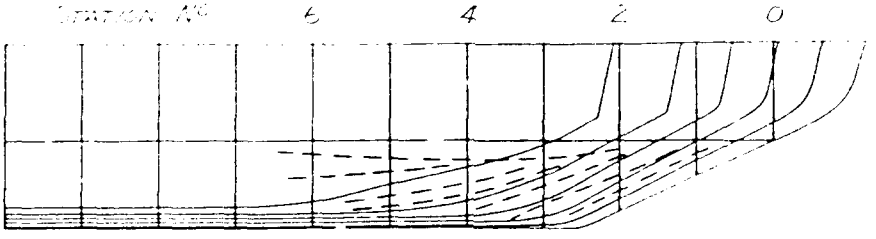

FIGURE 7-2, Flow Streamline Comparison

BOW 3 at 12.5 KNOTS

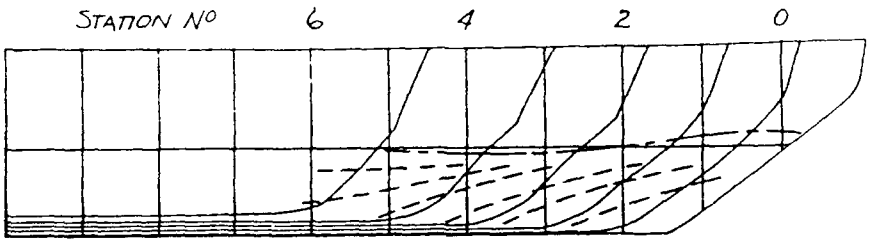

NOTE:
(1) Proposed bottom mapping sonar system location: between Stations 5&6

BOW 5 at 12.5 KNOTS

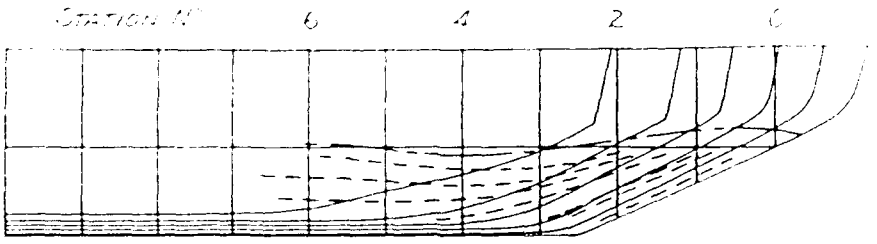

and 6. As Figure 7-1 shows, this would effectively keep much of the bubbles or ice away from the sonar system.

At the high end of the speed range for sonar operation, 12.5 kts, both the observed effects and the reason for them become much clearer. A substantial bow surface wave profile has developed, which is of minimum amplitude in Bow 3, and progresses to a maximum amplitude in Bow 5. Bow 4 and Bow 5, the two fullest, had the most pronounced bow waves, almost definitely an effect of the increasing waterline angles.

Bow 3 again has streamlines which tend to cross the buttocks and could cause some problems with the operation of the sonar. In Bow 5, it becomes evident why the streamlines tend to follow the buttocks or even cross them flowing up the ship's side at this speed. The generated surface wave has its first crest at Stations 0-2, a trough near Stations 3-5, and begins to move into the next crest at Stations 5 and 6. This trough and subsequent crest are so much more pronounced in Bow 5, that the surface wave tends to "pull" the streamlines up with it and across the buttocks towards the free surface in the vicinity of Stations 5 and 6. This would almost certainly serve to significantly decrease interference with the sonar as compared to the finer bows at 12.5 kts. The usual penalty of fuller bows was discussed in Chapter 5 (i.e., increased wave resistance), but as quantitative analysis at 15 kts showed, the EHP increase in Bow 5 at this speed is bearable considering the advantages gained in other areas of

performance. The distinction between them at 12.5 kts is even less clear than at 15 kts (See Figure 5-2, the comparison of still water EHP for each bow). Bow waves had an unexpected benefit.

There is one other observation made during the flow visualization tests which was unrelated to the flow and which occurred for all bows at all speeds. After each run, the carriage was returned at a low speed to the start position, where waves were allowed to dissipate before the next test. This allowed a chance to observe the flow while backing at a low speed. During backing, especially when the surface of the water was still unsteady, the stern tended to slap against the free surface, causing bubbles to form which flowed along the bottom of the aft part of the ship, until finally being swept out near the beginning of the parallel midbody. The significance of this flow condition, if any, is not known; the author feels it worthwhile to note it for future review. The behavior of the stern, with the transom above the free surface at design draft, suggests two potential problems - the first dealing with the possibility of slamming in heavy seas, and the second being these flow-related problems. Their relevance on the design of the ship must be considered.

8. CONCLUSIONS

Variations in the flare angle, β, and the waterline angle, α, of a ship with a traditional icebreaking bow have been shown to cause changes in the open-water powering, seakeeping, and hydrodynamic flow characteristics of that ship. In particular, analysis of the experimental data indicates that:

(1) Bow angle variations may result in a reduction of still water effective horsepower by as much as 10% (Bow 3) at 15 knots. The fullest bow, Bow 5, had a modest EHP increase of 2.2% with respect to the parent hull form at 15 knots.

(2) As β and α are increased, the pitch, heave, relative bow motion at Station 2 and added resistance in waves responses all decrease at both speeds and corresponding seastates. Bow 5 had reductions from 40 to 50% with respect to the parent hull form at 15 knots in a significant wave height of 8 feet.

(3) Deck wetness becomes an increasing problem as the center of buoyancy moves forward. Possible solutions include addition of a bulwark, or a softening of the hard chine to allow the flare to extend up to the deck-at-edge.

(4) The possibility of slamming exists on both the flat transom stern and the relatively flat run leading to the transom when the ship is experiencing heavy pitch motions.

(5) A tendency exists for the generated surface wave to sweep flow streamlines away from the planned bottom mapping sonar location between Stations 5 and 6, especially in Bows 4 and 5. Such an effect could prevent ice and/or bubbles from a bubbler hull lubrication system from interfering with the sonar.

(6) A possibility exists for flow to sweep bubbles, debris, or ice under the stern of the ship when backing down.

Based on these results, it has become clear that an icebreaker's flare and waterline angles may be increased, providing the benefits of: greater icebreaking capability, much better seakeeping overall, less acoustic interference with a bottom mapping sonar at the range of operating speeds, and all with only a modest increase in still water powering requirements at a typical operating speed, 15 knots. Although the finest bow, Bow 3, had improved seakeeping responses, it already represents the light end of the design range for icebreakers. Changing angles in the direction of Bow 5 yields the best of many worlds, with only slight disadvantages.

As long as these modifications are applied to ships with traditional icebreaking bows, they should be applicable for most ice-capable ships. The positive effects of increased waterline flare on seakeeping are becoming more widely accepted. The destroyer, ARLEIGH BURKE (DDG 51), is an example of this principle being put into practice.

9. SUGGESTIONS FOR FUTURE RESEARCH

Although the present systematic variation of a traditionally designed icebreaker has addressed the effect of varying the bow form angles, α and β, on calm water powering, and the seaway responses of pitch, heave, relative bow motion, and added resistance in waves, there is a need to continue this research into other aspects of icebreaker performance. Using the same models, analysis of other seakeeping responses such as slamming pressures and vertical accelerations at the center of gravity and at the bow would be useful in order to more fully describe the effects of the systematic variations on open-water seakeeping. Additionally, a series of variations using the same parent could be used to more effectively quantify methods to decrease deck wetness as the center of buoyancy moves forward and displacement increases.

Another major problem affecting the performance of icebreakers in open-water is their roll characteristics. The present series would not be suitable for investigating roll, as factors which most influence roll, including the maximum beam and the midships section shape, would be better varied in another series. Experimentation to evaluate methods to improve roll response while still remaining within the normal icebreaker design ranges would be very useful.

Although extensive steps were taken to insure that all bow variations kept the hull within standard icebreaking design ranges, in-ice testing of the models to confirm that they remain effective icebreakers would be of great benefit. In particular, such testing should confirm that Bows 2,4, and 5 are in fact better icebreakers than their parent.

ACKNOWLEDGEMENTS

The author of this Trident Scholar Report wishes to gratefully acknowledge the assistance of the following people:

Mr. Peter Zahn and Mr. Daniel Bagnell for their advice on the selection of a parent hull, and the later provision of the lines for T-AGS OCEAN (ICE).

Mr. Tom Price of the U.S. Naval Academy's Technical Support Department for the construction of the five forebodies and one stern involved in this project.

Mr. John Hill, Mr. Stephen Enzinger, Mr. Don Bunker, and the rest of the staff of the Naval Academy Hydromechanics Laboratory for their assistance in completing the experimentation and analysis.

Ms. Nancy Anderson, also of the Naval Academy Hydromechanics Laboratory, for assisting me with all the computer applications necessary to complete this project, especially with the use of FASTSHIP.

Most importantly, Dr. Roger Compton and Dr. Bruce Nehrling who served as my Trident Scholar Advisors for this project.

REFERENCES

[1] Lewis, Jack W., et al., Predicting Icebreaking Capabilities of Icebreakers, Naval Engineering Division Report No. 2 (CG-316-2), Washington: Office of Engineering, USCG, May 1969, p. 9.

[2] Melberg , L.C., et al., "The Design of Polar Icebreakers", SNAME Spring Meeting, 1-3 Apr 1970 , p. 2-5.

[3] Zahn, Peter, "The Estimation of Icebreaker Powering and Propulsion", MA-RD-840-89006 Report, Washington: Maritime Administration, Aug 1987.

[4] Melberg, L.C., et al., "The Design of Polar Icebreakers". SNAME Spring Meeting, 1-3 Apr 1970, p. 2-6.

[5] Zahn, Peter, "The Estimation of Icebreaker Powering and Propulsion", MA-RD-840-89006 Report, Aug 1987, p. 3-7.

[6] Melberg, L.C., et al., "The Design of Polar Icebreakers", SNAME Spring Meeting, 1-3 Apr 1970, p. 2-5.

[7] Kashteljan, V.I., et al., Icebreakers, Trans. by USACRREL, 1973, Leningrad: Sudostroyeniye, 1972.

[8] Strasel, et. al, "Feasibility Studies for an Ice Capable Oceanographic Survey Ship - FY92 T-AGS OCEAN (ICE)", SNAME Chesapeake Section Meeting, 11 Dec 1990, p. 1.

[9] Advanced Marine Enterprises, Inc., Hull Form Angles - T-AGS OCEAN (ICE), Job 7210-22-5, 18 Jan 1990, p. 2.

[10] Strasel, Erik S., et al., "Feasibility Studies for an Ice Capable Oceanographic Survey Ship - FY92 T-AGS OCEAN (ICE)", SNAME Chesapeake Section Meeting, 11 Dec 1990, p. 9.

[11] Moton, Casey J., Enzinger, Stephen, Bunker Donald, "Systematic Series of Icebreaking Bow Shapes: Open Water Resistance and Head Seas Response Measured Data Base", USNA EW Report No. EW-6-91, April 1991.

[12] Lewis, Edward V. ed., Principles of Naval Architecture, Vol 2, SNAME, 1988, p. 7.

[13] Enzinger, Stephen, "Resistance Tests on U.S. Coast Guard Icebreaker Series", Report EW-10-85, U.S. Naval Academy Hydromechanics Laboratory, June 1985.

[14] Bhattacharyya, Rameswar, Dynamics of Marine Vehicles, New York, NY, John Wiley and Sons, Inc., 1978, p. 227.

[15] Bhattacharyya, Rameswar, Dynamics of Marine Vehicles, New York, NY, John Wiley and Sons, Inc.,1978, p. 224.

[16] Strasel, Erik S., et al., "Feasibility Studies for an Ice Capable Oceanographic Survey Ship FY92 T-AGS OCEAN (ICE)." SNAME Chesapeake Section Meeting, 11 Dec 90.

APPENDICES

LONG CRESTED HEAD SEAS
MOTION RESPONSE SPECTRA FOR BOW 5
AT A SPEED OF 14.98 KNOTS
IN SEA STATE 4

ITTC (ONE PARAMETER)

SIG. WAVE HEIGHT = 8.000 ft
WIND SPEED = 20.780 Kts

ENCOUNTER FREQ. (rad/s)	ENCOUNTER SEA SPECT. (ft^2-s)	RBM SPECTRUM (ft^2-s)	HEAVE SPECTRUM (ft^2-s)	PITCH SPECTRUM (deg^2-s)	RES.(WAVES) SPECTRUM (lb-s)
0.0997	0.000E+00	0.000E+00	0.000E+00	0.000E+00	0.000E+00
0.1993	0.000E+00	0.000E+00	0.000E+00	0.000E+00	0.000E+00
0.2990	0.000E+00	0.000E+00	0.000E+00	0.000E+00	0.000E+00
0.3986	0.155E-18	0.388E-23	0.151E-18	0.644E-20	0.000E+00
0.4983	0.169E-07	0.243E-09	0.160E-07	0.129E-08	0.000E+00
0.5979	0.374E-03	0.326E-04	0.343E-03	0.500E-04	0.000E+00
0.6976	0.356E-01	0.106E-01	0.302E-01	0.764E-02	0.000E+00
0.7973	0.341E+00	0.285E+00	0.250E+00	0.102E+00	0.000E+00
0.8969	0.110E+01	0.223E+01	0.637E+00	0.374E+00	0.000E+00
0.9966	0.203E+01	0.827E+01	0.915E+00	0.653E+00	0.000E+00
1.0962	0.274E+01	0.185E+02	0.945E+00	0.664E+00	0.000E+00
1.1959	0.310E+01	0.246E+02	0.674E+00	0.414E+00	0.000E+00
1.2956	0.316E+01	0.177E+02	0.279E+00	0.147E+00	0.000E+00
1.3952	0.301E+01	0.851E+01	0.781E-01	0.440E-01	0.000E+00
1.4949	0.276E+01	0.474E+01	0.173E-01	0.111E-01	0.000E+00
1.5945	0.247E+01	0.308E+01	0.223E-02	0.111E-02	0.000E+00
1.6942	0.218E+01	0.227E+01	0.000E+00	0.000E+00	0.000E+00
1.7938	0.191E+01	0.191E+01	0.000E+00	0.000E+00	0.000E+00
1.8935	0.166E+01	0.166E+01	0.000E+00	0.000E+00	0.000E+00
1.9932	0.145E+01	0.145E+01	0.000E+00	0.000E+00	0.000E+00

	RBM (ft)	HEAVE (ft)	PITCH (deg)	RES.(WAVES) (lb)
AVG OF 1/3 HIGHEST	12.322	2.470	1.96	0.00
AVG OF 1/10 HIGHEST	15.710	3.150	2.50	0.00

APPENDIX 6-1, Sample Output of Ship Motions Program
used to expand model TF's for pitch, heave, and RBM

BOW 1 at 5.0 KNOTS

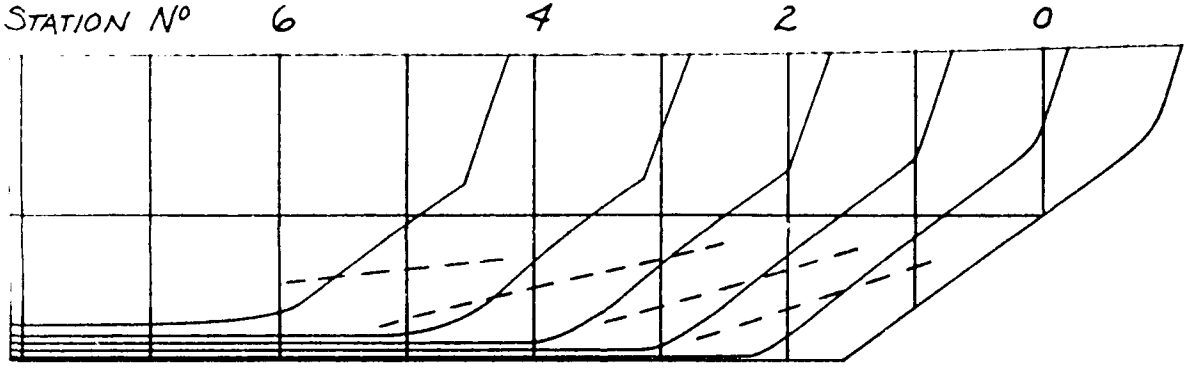

NOTES:
(1) Proposed bottom mapping sonar system location: between Stations 5&6
(2) No noticeable surface wave at this low speed

Appendix 7-1 (b), Flow Streamlines

BOW 2 at 5.0 KNOTS

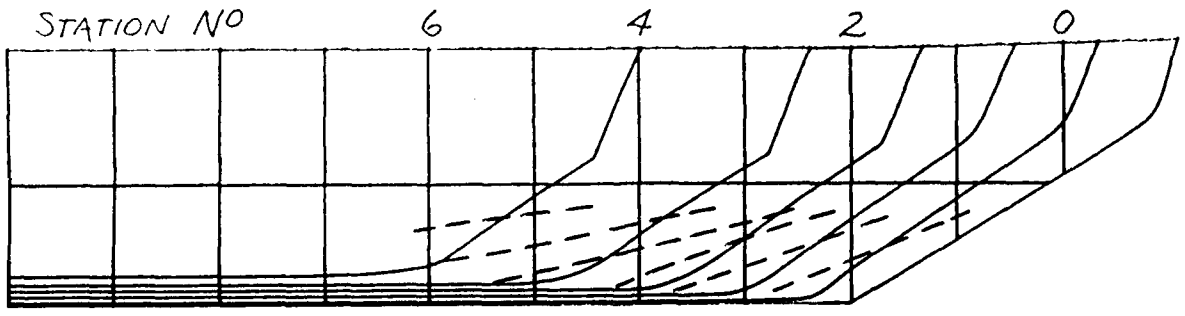

NOTES:
(1) Proposed bottom mapping sonar system location: between Stations 5&6
(2) No noticeable surface wave at this low speed

Appendix 7-1 (c), Flow Streamlines

BOW 3 at 5.0 KNOTS

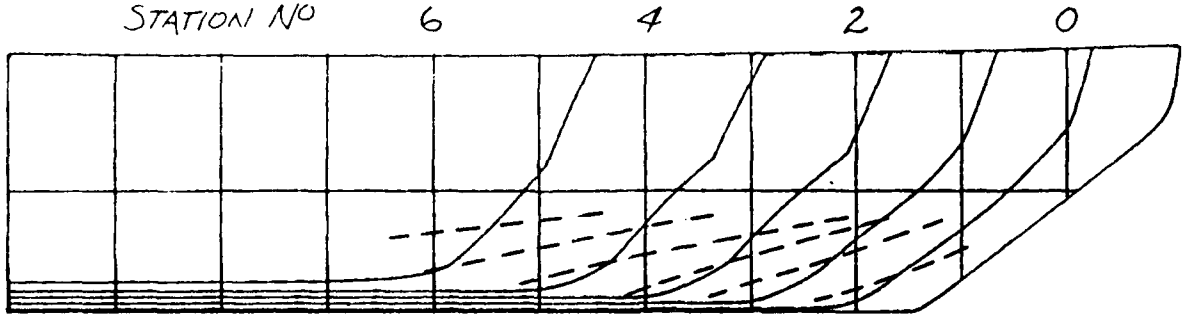

NOTES:
(1) Proposed bottom mapping sonar system location: between Stations 5&6
(2) No noticeable surface wave at this low speed

Appendix 7-1 (d), Flow Streamlines

BOW 4 at 5.0 KNOTS

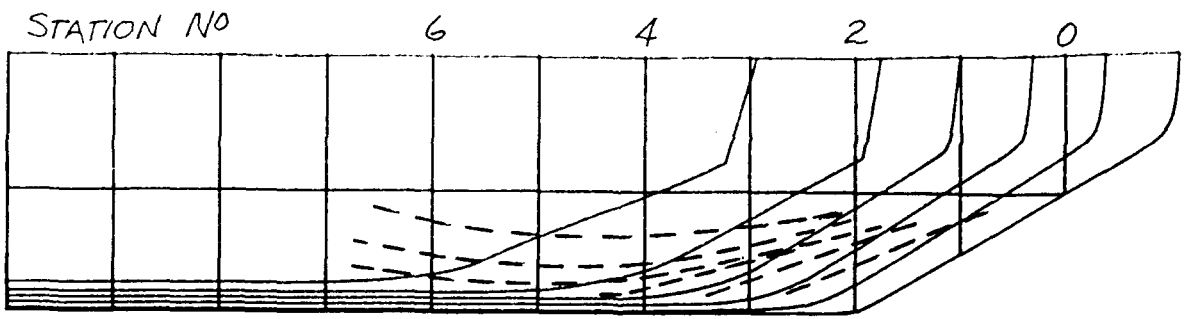

NOTES:
(1) Proposed bottom mapping sonar system location: between Stations 5&6
(2) No noticeable surface wave at this low speed

Appendix 7-1 (e), Flow Streamlines

BOW 5 at 5.0 KNOTS

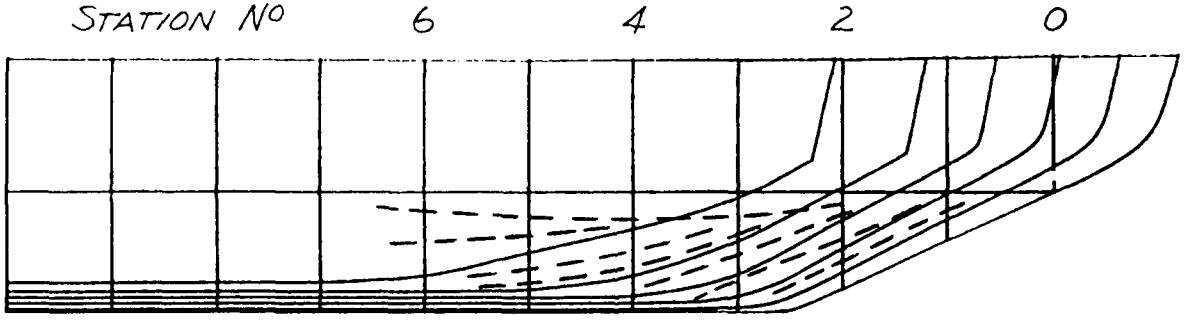

NOTES:
(1) Proposed bottom mapping sonar system location: between Stations 5&6
(2) No noticeable surface wave at this low speed

BOW 1 at 12.5 KNOTS

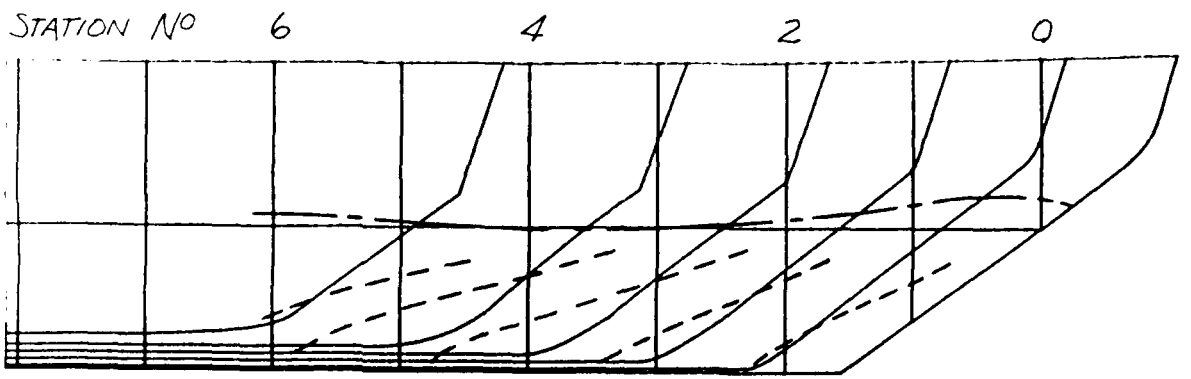

NOTE:
(1) Proposed bottom mapping sonar system location: between Stations 5&6

BOW 2 at 12.5 KNOTS

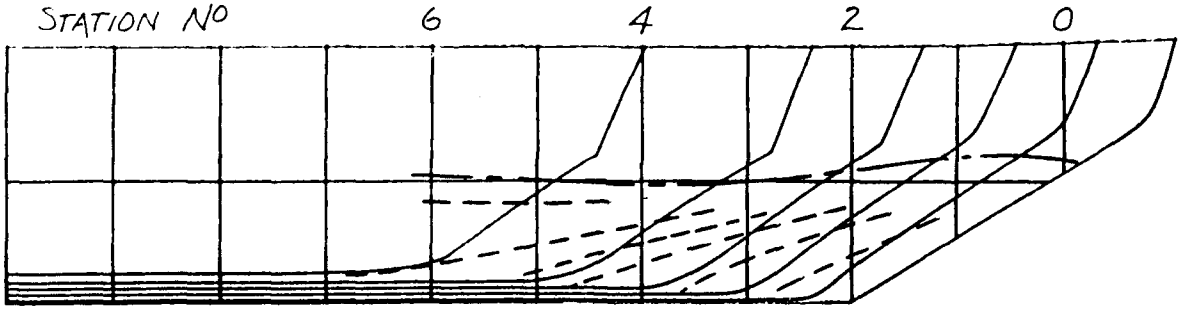

NOTE:
(1) Proposed bottom mapping sonar system location: between Stations 5&6

BOW 3 at 12.5 KNOTS

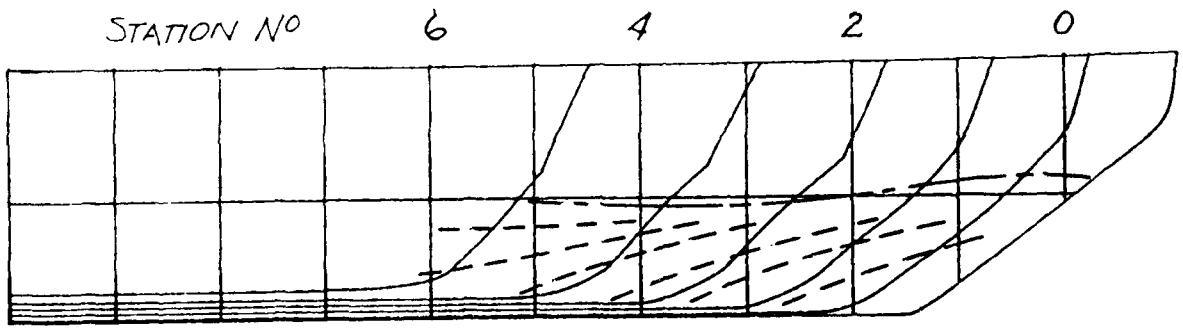

NOTE:
(1) Proposed bottom mapping sonar system location: between Stations 5&6

BOW 4 at 12.5 KNOTS

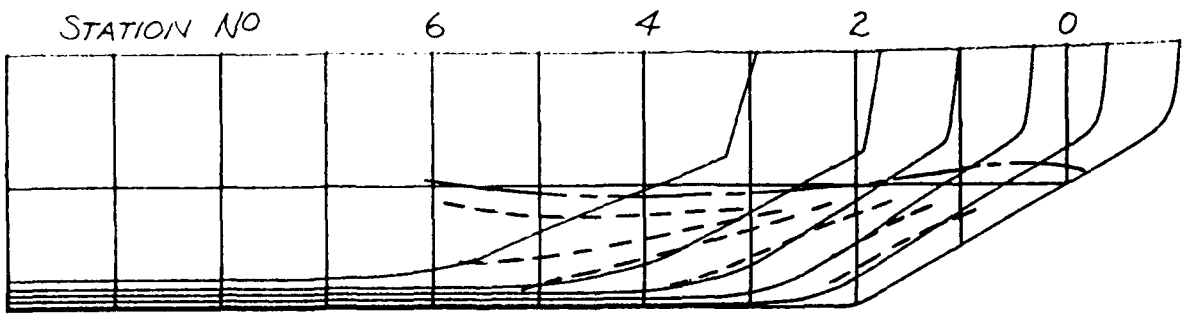

NOTE:
(1) Proposed bottom mapping sonar system location: between Stations 5&6

BOW 5 at 12.5 KNOTS

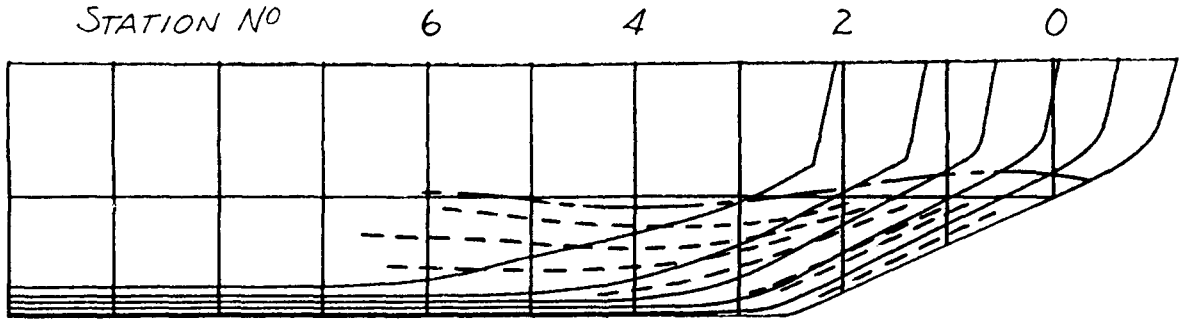

NOTE:
(1) Proposed bottom mapping sonar system location: between Stations 5&6